Potential Reemergence of Seasonal Soil Moisture Anomalies in North America

Sanjiv Kumar

School of Forestry and Wildlife Sciences, Auburn University, Auburn, Alabama

Matthew Newman and Yan Wang

Cooperative Institute for Research in Environmental Sciences, University of Colorado Boulder, and Physical Sciences Division, NOAA/Earth System Research Laboratory, Boulder, Colorado

Ben Livneh

Cooperative Institute for Research in Environmental Sciences, and Department of Civil, Environmental, and Architectural Engineering, University of Colorado Boulder, Boulder, Colorado

ABSTRACT

Soil moisture anomalies within the root zone (roughly, soil depths down to ~0.4 m) typically persist only a few months. Consequently, land surface–related climate predictability research has often focused on subseasonal to seasonal time scales. However, in this study of multidecadal in situ datasets and land data assimilation products, we find that root zone soil moisture anomalies can recur several or more seasons after they were initiated, indicating potential interannual predictability. Lead–lag correlations show that this recurrence often happens during one fixed season and also seems related to the greater memory of soil moisture anomalies within the layer beneath the root zone, with memory on the order of several months to over a year. That is, in some seasons, notably spring and summer when the vertical soil water potential gradient reverses sign throughout much of North America, deeper soil moisture anomalies appear to return to the surface, thereby restoring an earlier root zone anomaly that had decayed. We call this process "reemergence," in analogy with a similar seasonally varying process (with different underlying physics) providing winter-to-winter memory to the extratropical ocean surface layer. Pronounced spatial and seasonal dependence of soil moisture reemergence is found that is frequently, but not always, robust across datasets. Also, some of its aspects appear sensitive to spatial and temporal sampling, especially within the shorter available in situ datasets, and to precipitation variability. Like its namesake, soil moisture reemergence may enhance interannual-to-decadal variability, notably of droughts. Its detailed physics and role within the climate system, however, remain to be understood.

1. Introduction

Long-term (multiyear) droughts occur worldwide, particularly in semiarid to arid regions such as the southwestern United States, the Sahel, and Australia (Cheng et al. 2016; Evans et al. 2017; Held et al. 2005). In

North America, the recent California drought (2012–15) resulted in billions of dollars of economic losses and severe stress on ecosystem productivity (Asner et al. 2016; Howitt et al. 2015). Over the past century the U.S. Great Plains has experienced both costly droughts and extended pluvial periods (Livneh and Hoerling 2016). Improved understanding of mechanisms behind the potential predictability of long-term phenomena mediated by the land surface, including drought, may better inform natural resource planning decisions.

Drought is triggered by a substantial precipitation deficit that can even develop in a matter of days to weeks (Hoerling et al. 2014; Mo and Lettenmaier 2015), with surface feedbacks including antecedent conditions subsequently intensifying and prolonging the resulting soil

---

ᵃ Denotes content that is immediately available upon publication as open access.

✎ Supplemental information related to this paper is available at the Journals Online website: https://doi.org/10.1175/JCLI-D-18-0540.s1.

Corresponding author: Sanjiv Kumar, szk0139@auburn.edu

moisture deficit (Lyon and Dole 1995; Oglesby and Erickson 1989; Otkin et al. 2016; PaiMazumder and Done 2016). Soil moisture and precipitation feedbacks in the Great Plains are asymmetric, with droughts driving higher precipitation variability than floods (Schubert et al. 2008). More generally, since soil moisture anomalies persist longer than atmospheric moisture anomalies, land processes contribute to both subseasonal (Koster et al. 2010, 2011) and seasonal (Guo et al. 2011; Kumar et al. 2014b; Paolino et al. 2012) climate predictability. Realistic soil moisture initializations also improve seasonal stream-flow and soil moisture forecasts (Orth and Seneviratne 2013), because of time-integration effects of soil moisture and snow processes at watershed scales (Wood et al. 2016).

"Soil moisture memory" refers to the degree of persistence (high memory) or dissipation (low memory) of a soil moisture anomaly through time (Koster and Suarez 2001). Numerous studies have found that memory in the surface soil ranges between about 2 and 4 months, both in observations (Amenu et al. 2005; Dirmeyer et al. 2016; Entin et al. 2000; Nicolai-Shaw et al. 2016; Orth and Seneviratne 2012; Vinnikov et al. 1996; Wu et al. 2002) and climate model simulations (Delworth and Manabe 1988; Koster and Suarez 2001; Seneviratne and Koster 2012; Seneviratne et al. 2006; Wu and Dickinson 2004). Theoretical estimates from soil water balance models yield similar values (Ghannam et al. 2016; Orth et al. 2013; Seneviratne and Koster 2012). This memory time scale is spatially dependent, and dry regions may have higher memory (~3 months) than wet regions (~1 month) (Rahman et al. 2015).

However, if surface soil moisture memory is on the order of months, then what accounts for long-term droughts and pluvials persisting beyond a season, even years, seen in both instrumental and paleo-proxy climate datasets and in model simulations (Ault et al. 2013; Cook et al. 2016; Cook et al. 2004; Herweijer et al. 2007; Kam and Sheffield 2016; Langford et al. 2014; Schubert et al. 2004; Seager et al. 2005; Wu and Kinter 2009)? One explanation is that atmospheric teleconnections from ocean basins (Hoerling et al. 2014; Nicolai Shaw et al. 2016; Routson et al. 2016; Wu and Kinter 2009), including the tropical Pacific (Cole et al. 2002; Hoerling and Kumar 2003; Schubert et al. 2008; Seager et al. 2005) and the extratropical Atlantic (McCabe et al. 2004; Schubert et al. 2004), drive long-term variations in precipitation. Even without oceanic forcing, extended periods with substantial precipitation anomalies could occur randomly through natural variations of weather alone (Hasselmann 1976; Langford et al. 2014; Stevenson et al. 2015) despite its generally short memory (Chikamoto et al. 2015; Schubert et al. 2016; Seager et al. 2015). While historical "megadroughts" (Woodhouse and Overpeck 1998) may additionally be forced by changes in volcanism

and solar insolation (Seager et al. 2007; Woodhouse and Overpeck 1998), they too likely reflect internal climate variability (Ault et al. 2018; Coats et al. 2016; Seager et al. 2007, 2008).

Even so, observational and model studies have consistently identified multiseasonal to multiyear memory in deep soil moisture and groundwater, which could also contribute to long-term climate predictability including drought (Amenu et al. 2005; Bellucci et al. 2015; Bierkens and van den Hurk 2007; Entekhabi et al. 1996; Xia et al. 2014) and pluvials (Schubert et al. 2008). For example, the memory time scale of Illinois soil moisture anomalies below about 1-m depth is close to a year (Amenu et al. 2005). Soil moisture stored in the wet season supports plant growth in the subsequent dry season (Huete et al. 2006; Markewitz et al. 2010; Yan and Dickinson 2014). Groundwater might impact evapotranspiration through upward soil water flux (Fan and Miguez-Macho 2010; Miguez-Macho and Fan 2012) so recycling of evaporative flux could contribute to multiyear persistence in rainfall anomalies (Bierkens and van den Hurk 2007). Mahanama et al. (2012) found that 1 October initialization of soil moisture contributes to skill in streamflow forecasts at longer lead times, such as the following spring and summer seasons. Schubert et al. (2004) suggested that Great Plains drought is partly a consequence of year-to year "deep" soil memory. Analyses of megadroughts have also suggested that land surface memory must significantly contribute to their persistence (Ault et al. 2018; Cook et al. 2016). These studies all suggest that land surface memory is effectively greater than just a few months.

What seems to have received less attention is just how longer memory within the deep layer is communicated to the shorter-memory surface layer to sustain climate anomalies like long-term drought. Figure 1 both illustrates this issue and a potential explanation, showing a vertical cross section of the evolution of anomalous soil moisture during the 1988–89 Illinois drought, based on Illinois Climate Network (ICN) in situ data (Hollinger and Isard 1994). The spring 1988 precipitation deficit induced a dry surface soil moisture anomaly that propagated downward during summer 1988. While anomalies to a depth of ~40 cm decayed over a few months, as expected, beneath this depth the dry anomaly persisted throughout the following winter and spring. In spring 1989, even though precipitation was slightly above normal, surface soil moisture anomalies again became more negative. Interestingly, only afterward, in April, did a negative precipitation anomaly develop. Could the deep soil moisture anomaly have had any role in these surface changes, such as by driving anomalously dry surface soil conditions to recur in the second year?
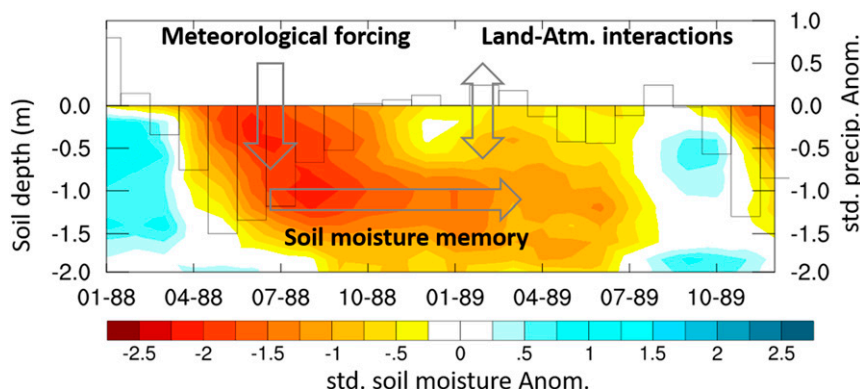
FIG. 1. Evolution of Illinois soil moisture standardized anomalies during and after the 1988 drought, averaged over Illinois Climate Network (ICN) observations. Contour interval is 0.25 standard deviation. Also shown are the standardized precipitation anomalies (bars) for each month.

This example is reflected in the overall ICN statistics. Figure 2a shows the autocorrelation function of Illinois springtime root zone soil moisture seasonal anomalies for 1985–2004. Here and in the remainder of this paper, we define the "root zone" as spanning depths of 0–0.4 m, the soil layer where typically two-thirds or more of the plant roots reside and also the layer with the highest seasonal variability (Ghannam et al. 2016; Zeng 2001). The details of the calculation are deferred to section 3; they are not necessary to grasp the main point here. As expected from a first-order Markov process, the autocorrelation function initially decays exponentially toward zero, with an e-folding time scale of about 4 months, consistent with previous studies discussed above. However, for longer lags the autocorrelation does not remain near zero but instead increases to become significantly positive again for leads of 13–15 months. That is, even as Illinois anomalous root zone soil moisture was uncorrelated from spring to the subsequent fall, it was significantly correlated from one spring to the next.

In fact, the annual cycle of the autocorrelation function (Fig. 2c) shows that while root zone soil moisture anomalies initially last only a few months, they recur in the subsequent spring (diagonal line), no matter the base season of the autocorrelation function. Yet no significant recurrence is apparent for precipitation (Figs. 2b and 2d). Together with Fig. 1, these results suggest that some springtime process might have partially restored prior soil moisture anomalies within the root zone by bringing back the memory of the previous year stored in the soil layer below. We call such a seasonally dependent process *soil moisture reemergence*, in analogy with a similar seasonally varying process (albeit with different underlying physics) that provides

long-term memory to thermal anomalies within the surface layer of the extratropical oceans (Alexander and Deser 1995; Alexander et al. 1999; Deser et al. 2003) and appears responsible for a substantial fraction of the variance of the Pacific decadal oscillation (PDO; Mantua et al. 1997; Newman et al. 2016).

Our immediate aim in this paper is to begin developing the following soil moisture reemergence hypothesis: deep layer soil moisture acts as a memory reservoir with significantly greater memory, ranging from several months to a year or longer (Amenu and Kumar 2008), than is typically present either in the root zone or in daily weather. Deep anomalies can interact with root zone soil moisture. If this interaction exists year-round, it may be expected to generally lengthen root zone memory time scales. However, when the connection is mediated by seasonally varying processes such as changes in snow cover, vegetation, and land–atmosphere coupling, then the root zone memory will generally be shorter except during seasons when the interaction with the deeper layer is pronounced, leading to soil moisture reemergence.

We would like to start by investigating how observations may constrain the proposed reemergence process and its possible physical mechanisms, examining the seasonal, regional, and depth dependence of soil moisture memory and its relationship to precipitation. This means going beyond earlier analyses of soil moisture memory, by determining the autocorrelation function of anomalous soil moisture over time intervals as long as two years. Unfortunately, the long-term, in situ soil moisture observations needed to study this phenomenon are limited. Therefore, much of this study involves evaluating long-term soil moisture memory and potential reemergence in various land data
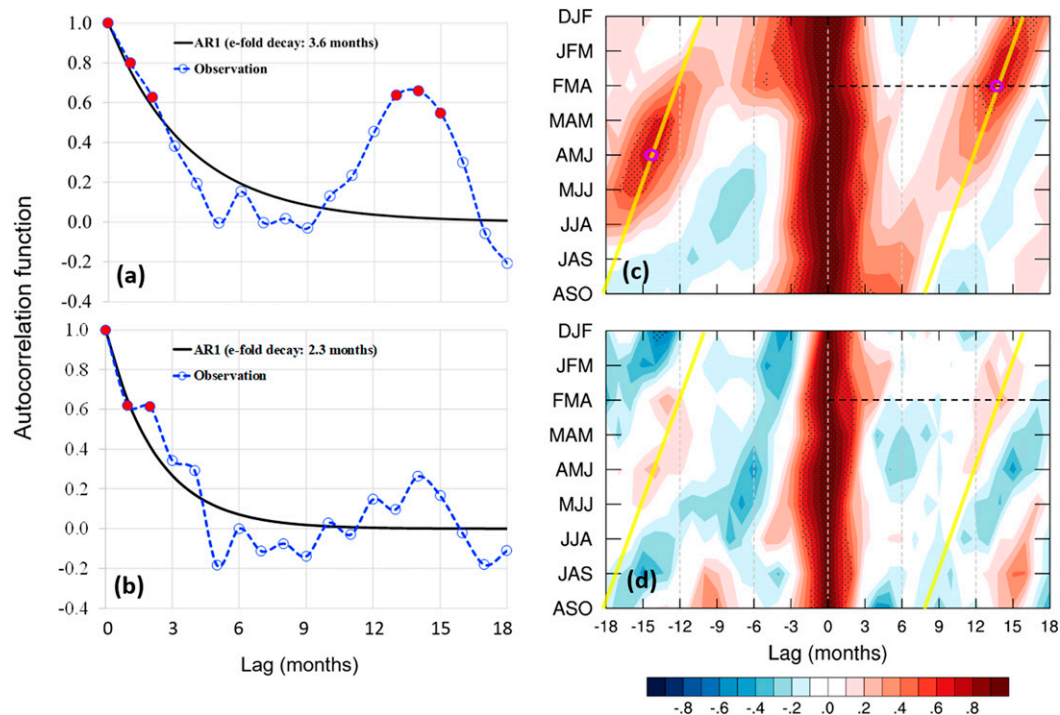
FIG. 2. Autocorrelation function of anomalous Illinois root zone (0–0.4-m depth) soil moisture and precipitation. Indices are determined from statewide averages of Illinois Climate Network (ICN) observations for 1985 to 2004, as described in the text. Anomalies are departures from the monthly seasonal cycle, smoothed with a 3-month running mean. (a),(b) Autocorrelation of springtime root zone soil moisture and precipitation, respectively. In both panels, autocorrelation lag is measured from the base FMA (February–April) anomalies; so, for example, a lead of 6 months represents the correlation between FMA and the subsequent ASO season. Dashed blue lines show the observed autocorrelation functions; solid black lines show exponential decay, where the decorrelation (e-folding) time scale is determined from a fit to the entire autocorrelation function. The red dots indicate values that are significantly different (95% confidence interval; see section 3c) from zero. (c),(d) Annual cycle of the autocorrelation function for 3-month running mean root zone soil moisture and precipitation anomalies, respectively. The month ordinate indicates the time of the base season, and the abscissa shows the lead/lag. For example, the (−13, MAM) value in (c) indicates the correlation of MAM root zone soil moisture anomaly with the previous year's FMA root zone soil moisture anomaly (i.e., 13 months earlier); the (14, FMA) value (magenta oval) indicates the correlation of FMA root zone soil moisture anomaly with the root zone soil moisture anomaly in the next year's AMJ season (i.e., 14 months later). The diagonal yellow lines therefore represent correlations with the previous FMA (subsequent AMJ) seasons, for any lead/lag. Correlation maxima along these lines are suggestive of reemergence. Note that both magenta ovals represent the 14-month lag correlation between FMA and the following AMJ (one oval forward and the other backward). The horizontal black dashed lines represent the location of the values in the blue dashed lines in (a) and (b). Note that in this and all subsequent plots, vertical dashed gray lines are drawn at 6-month intervals, and stippling represents the 95% confidence interval.

assimilation products. These products have their own well-known limitations, since they are derived from observed atmospheric forcing of the current generation of land surface models, but they yield results that appear reasonable on large scales (Dirmeyer et al. 2016). Since it is important to put the statistical analysis in a physical context, we first briefly introduce some potential mechanisms in section 2. Then, after summarizing all available soil moisture "datasets" that we analyze in section 3, the results of our analysis are presented in section 4. Finally, section 5 presents a summary and evaluation of our findings, including noting limitations of using datasets that are largely model-based and suggesting some avenues for further investigation.

2. Hypothesized soil moisture reemergence mechanisms

We first present some potential soil moisture reemergence mechanisms, in the context of the conceptual two-layer soil system model (Fig. 3):
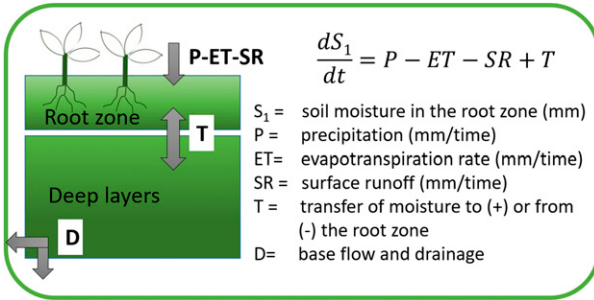
FIG. 3. A conceptual two-layer soil moisture model; see text for more details.

$$\frac{dS_1}{dt} = P - \mathrm{ET} - \mathrm{SR} + T, \qquad (1)$$

$$\frac{dS_2}{dt} = -T - D, \qquad (2)$$

where S_1 and S_2 are root zone (0–0.4 m) and deep layer (0.4–2 m) soil moisture, respectively. Here, we restrict our ''deep layer'' definition to only 2-m depth because this is where observations and data are readily available, but clearly soil and the water table below this depth may be relevant. Also, P is precipitation, ET is evapotranspiration, SR is surface runoff, and D is base flow and drainage; T represents coupling between the root zone and deep soil layers, defined to be positive when water flows from the deep soil to the root zone.

Darcy's law [(3)] governs water movement within a soil–plant–atmosphere continuous system as water moves from high to low potential (Goldsmith 2013):

$$\frac{dS}{dt} = -K\Delta\psi, \qquad (3)$$

where dS/dt is the rate of water flow (m s^{-1}) in the soil system, K is hydraulic conductivity (m s^{-1}), and $\Delta\psi$ is change in total soil water potential per unit length; for example, $\partial(\psi_{\mathrm{soil}} + z)/\partial z$ for water movement in the soil system. Figure 4a shows the soil moisture climatology and interannual variability from ICN data. The corresponding soil water potential ψ in Illinois shows a reversal from high to low potential between the root zone and deep layer in the late spring and summer seasons (see Fig. S1 in the online supplemental material).

It is widely accepted that water can move upward from the deep layer to the root zone following a soil water (matric) potential gradient (Green and Ampt 1911), which could occur when mean evapotranspiration exceeds precipitation in the growing season (Huete et al. 2006; Kumar and Merwade 2011; Kumar et al. 2014a; Markewitz et al. 2010; Sheffield et al. 2013; Yan and Dickinson 2014); that is, ET − P deficits are supplied by
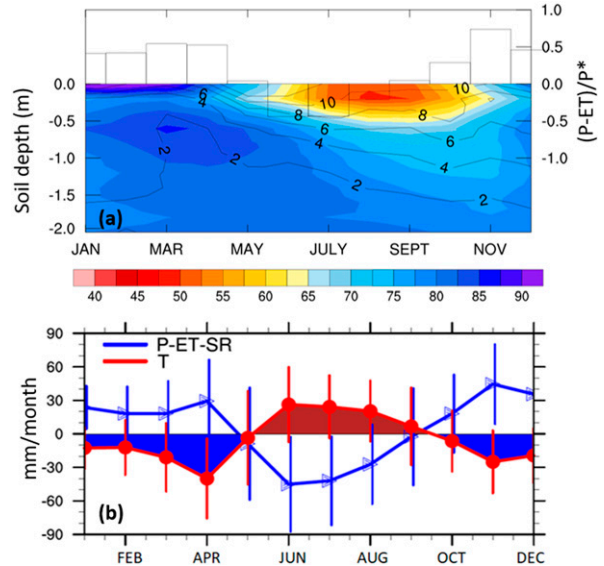

FIG. 4. Physics of soil moisture reemergence: a demand-driven hypothesis. (a) Soil moisture climatology, variability, and (P − ET)/P^* climatology: color shading shows monthly climatology of soil moisture in terms of percentage of saturation as a function of depth from the surface to 2 m. Line contours represent interannual variability using an estimate of one standard deviation from the ICN data. Bars shows P − ET climatology, normalized by annual average precipitation, using LDAS data from CLM. (b) An estimate of two major components: (P − ET − SR) and T, based on data from CLM. Error bars show interannual variability using an estimate of one standard deviation. Note the major contribution of T in the summer season. Units are mm month^{-1}. P^* is annual average precipitation.

the soil moisture storage available from previous seasons. Upward moisture fluxes on the basis of soil moisture gradients have been observed in nature (Scanlon 1992) and corroborated by models (Scanlon and Milly 1994), although these types of assessments have not been done over long periods or large areas. Examples of physical mechanisms that might drive water upward include 1) hydraulic redistribution, which is water movement from deep wet soil to dry shallow soil through the root system in the absence of transpiration demand (Lee et al. 2005; Meinzer et al. 2004; Neumann and Cardon 2012; Ryel et al. 2003; Ryel et al. 2002); 2) deep root plant water uptake, where deeper-rooted plants can access deep layer (and therefore higher memory) soil water (Huete et al. 2006); and 3) a shallow groundwater table position, which can contribute to the evaporative demand through capillary rise especially during droughts (Gao et al. 2017; Rizzo et al. 2018).

Figure 4b shows the climatology of various terms in (1) from an offline land surface model simulation (CLM, discussed later), which suggests that T constitutes a major portion (brown shading) of P − ET − SR deficits
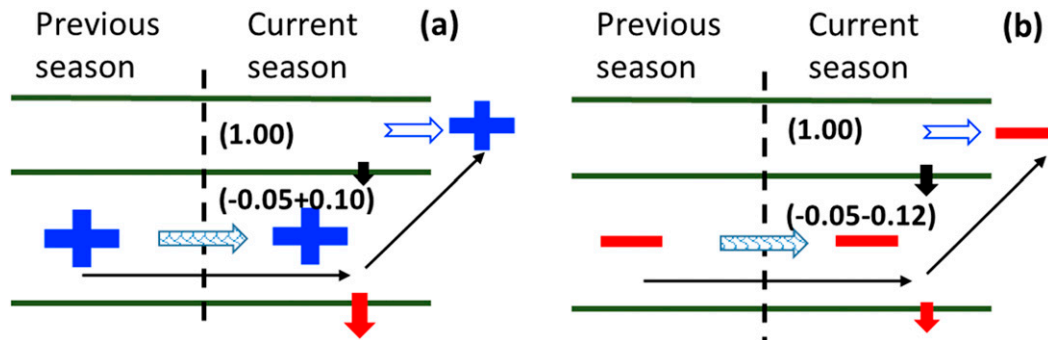
FIG. 5. Physics of soil moisture reemergence: anomaly propagation hypothesis. Both panels depict the conceptual two-layer soil model of Fig. 3, with anomalous soil moisture conditions and the total soil water potential (soil matric potential and gravitational potential with reference at 2-m depth) with anomalous soil moisture in the deep layer and (without loss of generality) climatological conditions in the root zone. (a) A deep layer wet anomaly would lead to a smaller potential gradient between the root zone and the deep layer and consequently a reduced magnitude of T, resulting in a wet anomaly developing in the root zone. (b) A deep layer dry anomaly would lead to larger potential gradient between the root zone and the deep layer and consequently an increased magnitude of T, resulting in a dry anomaly developing in the root zone. Numbers in the parentheses ($X \pm Y$) show the total soil water potential (meters of water) using ICN data for FMA season, where X represents the climatological mean value and Y represents one standard deviation of interannual variability. The hatched horizontal arrow in the deep layer represents the transfer of memory from the previous season to the current season. Filled thick black arrows show total water movement from root zone to the deep layer below. Filled thick red arrows show the drainage term. See text for further explanation.

in the summer, as well as contributing to the recharge of deep soil moisture during winter and early spring. Importantly, there are no direct observations of T; rather, it can be inferred as a difference term between soil moisture observations at two depths. Given a lack of long-term, high-quality observations needed for T (ICN notwithstanding), we must rely almost entirely on simulated soil moisture, which introduces uncertainty in the magnitude of potential reemergence.

A "demand-driven" soil moisture anomaly reemergence hypothesis might then act as follows: the root zone soil moisture anomalies contribute to deep layer anomalies during the wet season when the atmospheric supply exceeds the demand; that is, $P - \mathrm{ET} > 0$. The deep layer anomalies remain decoupled from atmospheric/evapotranspiration processes during winter and early spring because atmospheric demand is smaller than the atmospheric supply. As a result, the deep layer soil moisture has greater memory and smaller variability compared to the root zone (Fig. 4a). As the surface soil moisture dries out in late spring and summer, the soil water potential gradient reverses (i.e., the deep layers have higher soil water potential than the surface), leading to moisture transfer from the deep layer to the root zone.

It is also possible that reemergence can occur *without* upward water movement. This alternative "anomaly-propagation" hypothesis is illustrated in Fig. 5. Consider first the case of a pre-existing wet deep layer anomaly (left column). During the subsequent season, the rate of

downward water transfer to the deep layer would be reduced (i.e., there would be a negative T anomaly) because of a smaller-than-normal matric potential gradient between the root zone and deep layers. This would result in a net positive root zone soil moisture anomaly and an apparent upward propagation of the prior deep layer anomaly. Conversely, a dry deep layer anomaly would imply a larger-than-normal matric potential gradient between the root zone and deep layers, a positive T anomaly, and again apparent upward propagation of the deep layer anomaly (right column in Fig. 5b).

Clearly, both the proposed demand-driven and anomaly-propagation hypotheses are quite sensitive to how T depends upon all the other terms in (1), so the root zone anomaly development is likely considerably more complex than discussed here and may act differently in the presence of climate variability, surface heterogeneity, and land–atmosphere coupling. This two-layer heuristic model also oversimplifies the more complicated water movement through the soil column, including interactions with the aquifer below as well as lateral flow. How vegetation, both through its seasonal cycle of growth and sensitivity to soil moisture anomalies, impacts these mechanisms is also likely important. Still, fundamental physics (the Darcy law) and the observed matric potential gradients together provide possible mechanistic explanations for soil moisture reemergence.

Finally, K. Schaefer et al. (2007) suggested that freeze–thaw processes can lead to soil *temperature*

TABLE 1. Datasets used in this paper. Note that some datasets cover more years than were used.

Dataset	Years	Forcing	Notes
ICN: Illinois Climate Network	1985–2004	None (soil moisture measurements, using neutron probe); Hollinger and Isard (1994)	18 station average. Measurements are 1× monthly except 2× monthly in growing season
ARM, SCAN, and SNOTEL sites	Vary between 1998 and 2017 (see Fig. 13)	None (soil moisture measurements)	Measurements are daily
VIC-highres: High-resolution VIC (Livneh et al. 2015b)	1950–2010	Hydrologically consistent dataset for the conterminous United States, gridded at 1/16° latitude–longitude, derived from daily temperature and precipitation observations from approximately 20 000 NOAA Cooperative Observer (COOP) stations (Livneh et al. 2013)	Three-layer (variable depth) variable infiltration capacity (VIC) model, run at 1/16° resolution in 3-hourly increments
VIC-lowres: Coarse-resolution VIC (Livneh and Hoerling 2016)	1950–2010	Same as above	Three-layer fixed depths (VIC) model, run at 1/2° resolution in 3-hourly increments
CPC: Climate Prediction Center	1950–2010	Monthly data over the globe from CPC Precipitation Reconstruction over Land (Chen et al. 2002) and CPC Global Land Surface Air Temperature Analysis (Fan and van den Dool 2004)	One-layer hydrological model ("leaky bucket") with spatially constant parameters (Huang et al. 1996; van den Dool et al. 2003). Constant depth 1.6 m, run at 1/2° resolution, monthly
CLM	1950–2010	CRU3.2 + NCEP R1 temperatures/precipitation (CRUNCEP; Viovy and Ciais 2011)	NCAR Community Land Model (CLM) v4.5, 10 layers, constant depths, run at 1° resolution, 6-hourly increments (Oleson et al. 2013)
Noah (NLDAS-2)	1979–2010	NLDAS-2 forcing fields (NARR/PRISM, plus various corrections)	Land model used in NCEP operational models. Four layers, constant depths, 1/8° resolution, daily
Mosaic (NLDAS-2)	1979–2010	Same as for Noah	Land model originally used in NASA GCM; 1/8° resolution, daily
GLEAM (version 3)	1980–2015	Remote sensing–based soil moisture observations are assimilated using 3-layer soil moisture model in the Global Land Evaporation Amsterdam Model, 1/8° resolution, daily (Martens et al. 2017)	
SMERGE	1979–2015	Merging of satellite-based surface soil moisture with Noah (NLADS-2) root zone soil moisture data, 1/4° resolution, daily (Crow and Tobin 2018)	
MERRA2	1980–present	Daily precipitation totals were corrected using NOAA CPC unified gauge-based analysis (Chen et al. 2008) in the coupled atmosphere–land reanalysis system (Reichle et al. 2017)	Catchment hydrology model (Koster et al. 2000), root zone thickness 1 m, 1/2° resolution, 3-hourly

reemergence in cold regions: during the winter, soil temperature anomalies from the previous season are stored below the frozen surface, and then reappear at the surface during the subsequent thaw (also see Matsumura and Yamazaki 2012). A similar mechanism (perhaps also involving snowpack dynamics) might be relevant for moisture anomalies as well.

3. Data and methods

a. Soil moisture datasets and processing

Table 1 lists all the hydrology/land surface model datasets and in situ soil moisture measurements (and their acronyms) used in this study, including their period of record and their horizontal resolution. Below, we briefly describe these datasets. Given the short records of in situ and satellite soil moisture datasets, our methodology is limited to providing essentially a qualitative assessment of the "potential" existence of a reemergence phenomenon and its attributes, rather than a quantitative assessment of its magnitude. In this context, we focus on several multilayer soil moisture Land Data Assimilation System (LDAS) datasets that include different land surface models (LSMs) driven by observed meteorological forcing. This provides the longer records needed to study interannual to decadal variability. Note that LDAS datasets do not directly assimilate soil

moisture observations, however. Another important caveat is that the phenomenon of reemergence has not been directly built in to any of the models, nor has it been explicitly evaluated before, such that some models may be more or less suitable to simulate reemergence and that any characterization of reemergence from these models is likely to contain artifacts related to parameterization and discretization dependences.

We examined three LDAS methods with at least 60 years of data each. First, we used the Variable Infiltration Capacity model (VIC; Liang et al. 1994) in two configurations: 1) a hydrologically consistent high-resolution (1/16°) implementation, called VIC-highres, calibrated to streamflow observations (Livneh et al. 2013) and therefore providing an observationally constrained representation of soil moisture interactions relative to other model datasets; and 2) a lower-resolution (1/2°), spatially uniform soil depth implementation of VIC, called VIC-lowres, used by Livneh and Hoerling (2016) to simulate drought at scales comparable to GCMs, providing a useful contrast to the VIC-highres concerning model spatial resolution and calibration effects. Both use a three-layer soil moisture scheme, but VIC-highres uses spatially varying thicknesses dependent on its streamflow calibrations. Both are driven by gridded meteorological forcing data from approximately 20 000 NOAA Cooperative Observer stations (Livneh et al. 2013, 2015b), and both include a seasonally varying vegetation phenology and resolve both water and energy fluxes for the land surface and vegetation canopy layers. Additional experiments were made with the VIC-lowres in which the forcing is modified by fixing either precipitation or temperature to their climatologies (Livneh and Hoerling 2016) to explore the sensitivity of our results to anomalous meteorological forcing.

The VIC is contrasted with the Community Land Model version 4.5 (CLM; Oleson et al. 2013), an LSM with more sophisticated soil–plant–atmosphere interaction. The CLM has a coarser (1° × 1°) spatial resolution but also has a 10-layer fixed depth soil moisture scheme down to 3.5-m depth. It solves the one-dimensional Richard's equation within each soil column, which can share several plant functional types to account for vegetation heterogeneity at the surface. Plant functional types describe vegetation structure in terms of leaf properties, canopy heights, and root distributions (Bonan et al. 2002; Oleson et al. 2013). CLM also has a prognostic seasonal cycle of vegetation evolution, emergence and senescence of leaves, and vegetation heights based on the Biome-biogeochemical cycle model (Thornton and Rosenbloom 2005; Thornton et al. 2002). The soil moisture dataset is then generated by

forcing the CLM with meteorological observations based on the Climatic Research Unit (CRU)–National Centers for Environmental Prediction (NCEP) dataset, for the years 1901–2010. Despite differences between VIC and CLM, they produce similar snowpack dynamics (Chen et al. 2014) and share common physics assumptions: a two-stream canopy radiative transfer scheme, time-varying albedo, liquid water refreeze, and water transfer between snow layers.

Sensitivity to LDAS models is explored by analysis of two datasets from phase two of the North American Land Data Assimilation System (NLDAS-2) (Xia et al. 2012, 2014) based on the Noah and Mosaic models, covering the period since 1979. The Noah model has four soil layers with thicknesses of 10, 30, 60, and 100 cm. It provides land boundary conditions in the NOAA/NCEP coupled Climate Forecast System (Ek et al. 2003). Mosaic has three soil layers with thicknesses of 10, 30, and 160 cm, with the first two together comprising the root zone (Koster and Suarez 1996). Since both models receive identical observed atmospheric forcing, differences between these two datasets arise from model differences including their soil moisture parameterizations. We also examined the NLDAS-2 dataset based on the VIC model, but show the results obtained with the VIC-highres dataset instead since the differences have relatively minor impact on our results, and VIC-highres covers a longer period.

To provide a simplistic LSM for comparison, we used the Climate Prediction Center (CPC) soil moisture dataset, which uses observations to force a single-layer "leaky bucket model" (Huang et al. 1996; van den Dool et al. 2003) with an effective depth of 1.6 m. In essence, we have incorporated soil moisture datasets from a wide range of model parameterizations, from the most simplified with no vertical layers to complex (interactive vegetation phenology; CLM) and hydrologically calibrated (VIC) models.

More recently, remote sensing–based surface soil moisture observations have been assimilated to produce daily root zone soil moisture values at higher spatial resolution for the 1980–2015 period. Two such products are 1) the Global Land Evaporation Amsterdam Model (GLEAM), which assimilates soil moisture observations from different passive and active C- and L-band microwave sensors from European Space Agency Climate Change Initiative (ESA-CCI), using a three-layer water balance model where root zone depth is a function of land cover type; and 2) SoilMERGE (SMERGE), which was developed based on merging an NLDAS land surface model (Noah) dataset with the ESA-CCI satellite retrievals (Crow and Tobin 2018), using an exponential filter to convert surface soil moisture (0–5 cm) to root

zone soil moisture (0–40 cm) (Tobin et al. 2017). In addition, we included the Modern-Era Retrospective Analysis for Research and Applications version 2 (MERRA-2; Gelaro et al. 2017), a reanalysis product using observed precipitation to force the coupled land–atmosphere system, allowing near-surface temperature and humidity to be consistent with the precipitation correction and providing comparable performance to the corresponding LDAS-type simulations (Reichle et al. 2017). Finally, we determined an ensemble mean from all the above datasets for the common 1980–2010 period.

Given LSM/LDAS limitations, we might prefer to focus on in situ measurements, but such records are generally not over ~20 years in length, and most are shorter (Dirmeyer et al. 2016). The ICN covers 18 sites in Illinois from 1983 to 2004 (Hollinger and Isard 1994). Measurements were taken from 11 soil layers at depths of 0–10, 10–30, 30–50, 50–70, 70–90, 90–110, 110–130, 130–150, 150–170, 170–190, and 190–200 cm, generally once per month during the nongrowing season and twice per month (or more, in a few locations) during the growing season. Comparing LDAS and ICN datasets (see appendix A) shows that the VIC-highres best matched ICN, but that sparse ICN temporal sampling impacts our analysis.

Finally, we constructed monthly averages of daily soil moisture observations from sites that had at least 12 years of continuous monthly mean data to a depth of 40 cm. These include Ashton (ARM) in Kansas, Mandan (SCAN) in North Dakota, Adam's Ranch (SCAN) in New Mexico, Happy Jack (SNOTEL) in Arizona, Long Valley (SNOTEL) in Idaho, and Reynold's Creek (SNOTEL) in Idaho (see appendix A for more details, and Fig. A2 for their locations) (Bond 2005; Schaefer and Paetzold 2001; G. Schaefer et al. 2007). All in situ soil moisture observations were obtained from the International Soil Moisture Network (Dorigo et al. 2011, 2013).

b. Determining soil moisture seasonal anomalies

For each dataset, we smoothed the monthly averages with a 3-month running mean; this reduces intraseasonal variability but does not affect our results, as is illustrated in Fig. S2. We then computed the 3-month running mean anomalies by removing the long-term monthly climatology determined from the period of record. We tested the impact of linearly detrending the 1950–2010 datasets separately for each month but found the effects were small. Also, the trend since 1950 has both anthropogenic and natural sources (Solomon et al. 2011), and identification of only the external component is beyond the scope of this paper. Consequently, all analyses shown are based on data that were not detrended.

To focus on larger spatial scales, time series were computed by area averaging data within the boxes shown in Fig. 6 (see also Fig. A1), representing four regions: Illinois (also see appendix A), the Great Plains (GP), the Great Basin (GB), and the southwestern United States (SW).

c. Metrics

Most of the analysis in this paper involves the annual cycle of correlation functions for soil moisture and precipitation, determined separately for each 3-month season by correlating that season's anomalies with values at lags ranging from −24 to +24 months. These correlations were found both for a variable with itself [autocorrelation (AC)] and between two different variables [cross-correlation (CC)].

For comparison, note that the land surface integrates forcing by random weather and climate variability. Therefore, the simplest null hypothesis for soil moisture variability is red noise or a first-order Markov process (Amenu et al. 2005; Chikamoto et al. 2015; Delworth and Manabe 1988; Schlosser and Milly 2002), whose autocorrelation function ρ for a given lag τ is

$$\rho(\tau) = \exp\left(\frac{-\tau}{\tau_D}\right), \tag{4}$$

where τ_D is the decorrelation (or e-folding) time scale, also known as soil moisture memory. See appendix B for more details of the AC and CC calculations and their significance testing.

To develop a measure for evaluating reemergence, we first recall that the autocorrelation function in Fig. 2a declined from one to near zero but then increased at longer lags, reaching a maximum of 0.65 at a 14-month lag. This behavior can be captured by defining the recurrence time scale T_R as the lag at which the autocorrelation function reaches its first secondary maximum (i.e., 14 months in Fig. 2a). Note that T_R is only evaluated when the correlation value at this secondary maximum (or the recurrence magnitude) is statistically significant at the 95% level (appendix B), Importantly, T_R is a function of the starting season; that is, it measures how long it takes until an anomaly from a given season will recur. So, from Fig. 2b, for example, FMA soil moisture anomalies recur after about $T_R = 14$ months [in the second year April–June (AMJ) season], whereas AMJ soil moisture anomalies take $T_R = 12$ months to recur (also in AMJ). Since no information about subsurface soil moisture anomalies is used to compute T_R, we call it a measure of anomaly recurrence, not (necessarily) reemergence.
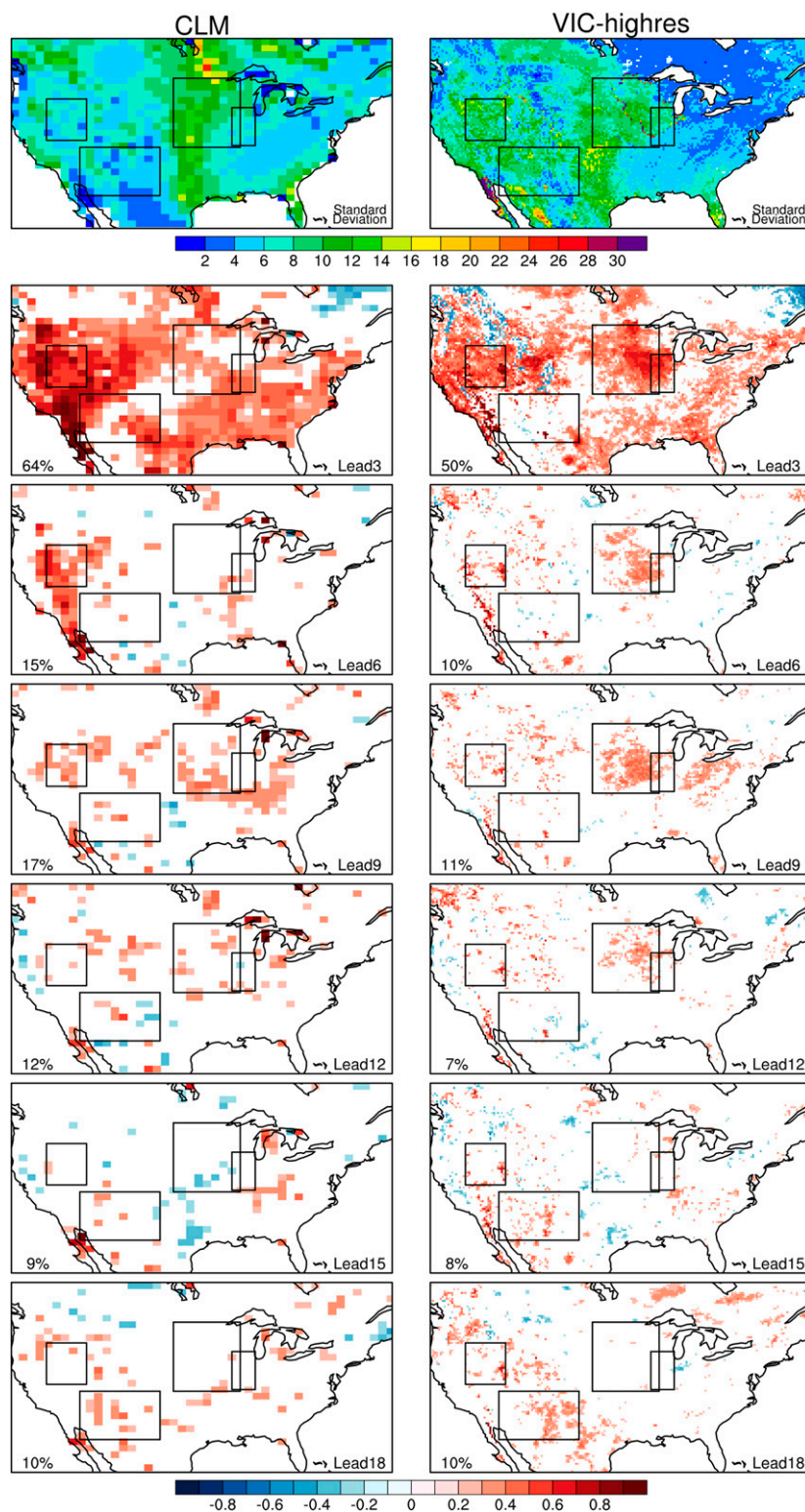
FIG. 6. (top) Root zone soil moisture standard deviation and (lower rows) lag correlation from 3 to 18 months, for MAM base season, 1950–2010, in the (left) NCAR CLM and (right) VIC-highres datasets. Only statistically significant autocorrelations (95% level) are shown using color scale in rows 2–7. Numbers in each panel show the percent of areal coverage of the significant autocorrelations. The outlines of boxes used to define the regional time series (see text and also Fig. A2) are also shown.

4. Results

a. Soil moisture memory and reemergence in North America

Figure 6 shows maps of springtime [March–May (MAM)] root zone soil moisture anomaly amplitude (i.e., standard deviation) for the CLM and VIC-highres datasets. [Fig. S3 shows results for the other three seasons.] Qualitatively similar large-scale features exist in both datasets, including pronounced maxima extending along a north–south direction through the Great Plains and in the southeast. However, clear differences in detail exist; for example, CLM variability is stronger in the northern Great Plains whereas VIC-highres variability is stronger in the Great Basin. These differences do not merely reflect the higher resolution effects (VIC-highres) but can result from differences in forcing, model structure, and soil moisture parameterizations.

Interestingly, the largest anomalies are not always the most persistent, as shown by the autocorrelation function maps for correlations between MAM anomalies and anomalies 3 [June–August (JJA)], 6 [September–November (SON)], 9 [December–February (DJF)], 12 (MAM +1), 15 (JJA +1), and 18 (SON +1) months later (Fig. 6). For example, at 3-month lead, there is substantially greater memory in the Great Basin and the Southeast and less in the Great Plains and southwestern United States. Despite this, at 9-month lead the Great Basin and Great Plains autocorrelation values are similar; in fact, the 9-month lead Great Plains autocorrelation increases considerably from its minimum at 6-month lead (cf. Fig. 2a). Likewise, the Southwest U.S. autocorrelation function reaches a secondary maximum at 18-month lead. Similar results are apparent in maps of autocorrelation functions lagged from JJA and SON anomalies (see Figs. S3a–c) except that these secondary maxima occur at different leads.

Note that these maps are field significant at all lags; that is, at least 5% of each map contains locally significant correlation at the 95% threshold. However, at some lags this is due to some statistically significant negative correlations, which could reflect precipitation forcing and not necessarily (at least not obviously) land effects.

To evaluate the potential for reemergence, we determined T_R (section 3c) from the CLM and VIC-highres datasets. The resulting maps (Fig. 7), based on the DJF, MAM, JJA, and SON seasons, have greater coverage than in Fig. 6 for the same significance value, which suggests that there is some uncertainty in the precise time scale of recurrence.

Overall, recurrence of root zone soil moisture anomalies is widespread throughout North America, albeit more pronounced in some regions and some seasons than others. Despite their differing resolutions, the two datasets share many notable features on larger scales. For example, within the Great Plains region recurrence values are quite similar in both areal extent and time scale for all seasons except JJA, where in the CLM they are more extensive and shifted westward relative to the VIC-highres. Recurrence in the Great Basin is present in both datasets but generally at much longer leads in the VIC-highres than CLM. Results appear to be notably dissimilar during JJA except in the Southwest where both datasets have fairly similar values [i.e., T_R is less (greater) than 10 months in the eastern (western) part of the box]. Also, in some areas (such as the southwestern and northeastern United States), significant values of T_R exist all or most of the year for both datasets, but their time scales change by season in a manner consistent with reemergence as described in Fig. 2b. For example, in the Southwest region T_R decreases by roughly 3-month increments (going from red to blue) in each panel from DJF through SON (Figs. 7a and 7d for CLM, and Figs. 7e and 7h for VIC-highres). On the other hand, some regions have significant values of T_R only for specific seasons. For example, in the Pacific coastal states, T_R seems primarily dependent upon winter soil moisture anomalies (cf. Figs. 7a and 7e, and to a lesser extent Figs. 7d and 7h), whereas T_R is most related to spring soil moisture in an area of the eastern Great Plains (Figs. 7b and 7f) that shifts westward (Figs. 7c and 7g) and substantially enlarges for summer anomalies in CLM. Further sensitivity of T_R to time period and dataset is shown in Fig. S4.

b. Regional soil moisture memory and reemergence

The variability statistics within the above datasets appear to agree better on larger spatial scales. This is also true for the other NLDAS2 products (Dirmeyer et al. 2016). To investigate reemergence on these larger scales, we constructed area-averaged time series for a few selected regions as described in section 3. We then determined both the root zone soil moisture and precipitation autocorrelation functions and the cross correlation between the root zone soil moisture and precipitation, all as a function of the annual cycle. Additionally, we determined the cross correlation of root zone soil moisture with the vertical profile of soil moisture for each season of the year. In the following, we show results using the CLM dataset since it has the most detailed vertical structure; similar analysis performed with the VIC-highres dataset yielded generally similar results (see section 4c).

The annual cycle of the root zone soil moisture autocorrelation function for the SW time series (Fig. 8a) shows its memory more than doubled (from ~3 to ~8
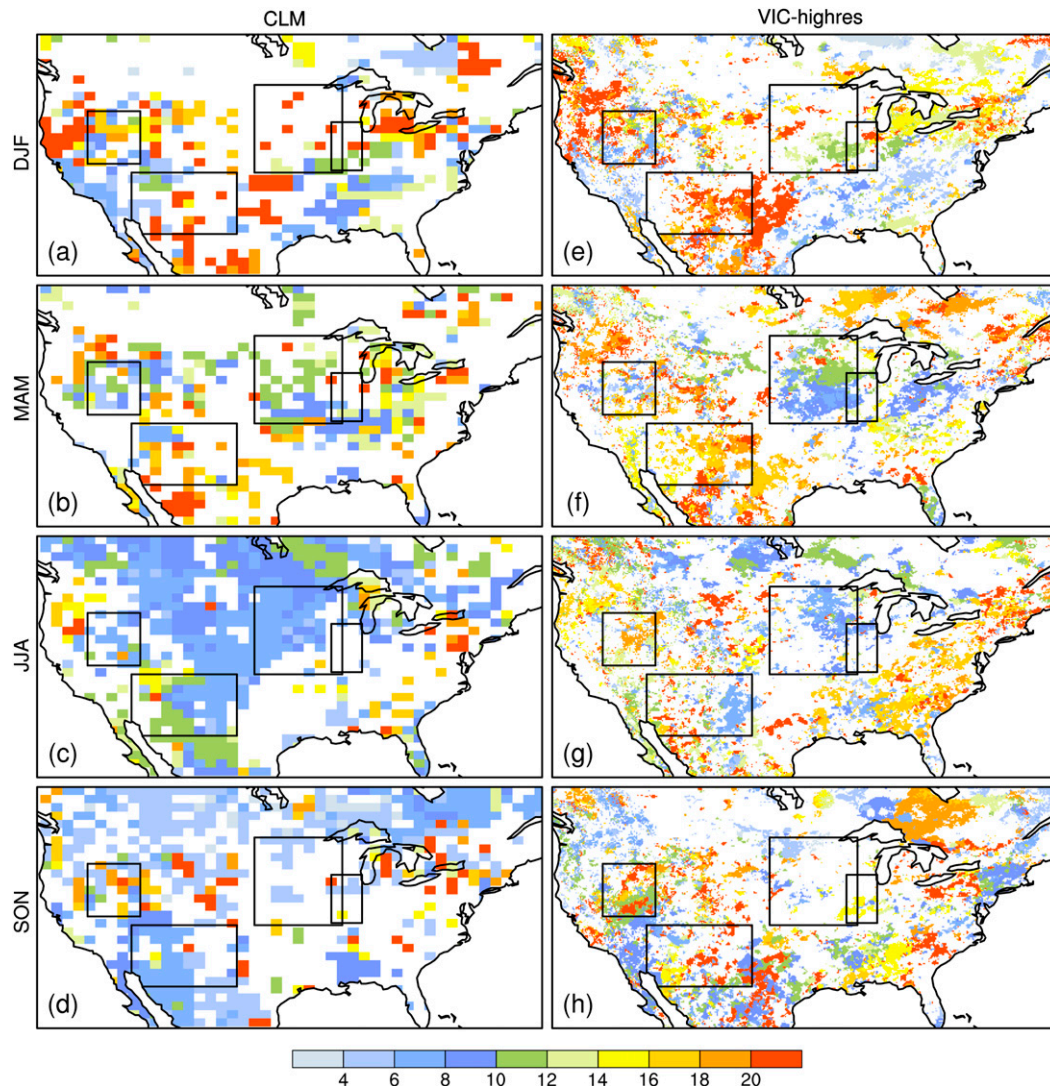
FIG. 7. Recurrence time scale T_R for root zone anomalous soil moisture in DJF, MAM, JJA, and SON base seasons, 1950–2010. Only values of T_R for which the recurrence magnitude is significant at the 95% level are shown. (left) T_R maps determined from CLM data for (a) DJF, (b) MAM, (c) JJA, and (d) SON. (right) As in left, but for VIC-highres for (e) DJF, (f) MAM, (g) JJA, and (h) SON. The outlines of boxes used to define the regional time series are also shown.

months) between spring and late fall. For autocorrelation functions starting from summer and early fall months, a secondary maximum extends diagonally from an 8-month lag for SON to a 12-month lag for MJJ. That is, significant autocorrelation values recur during the subsequent summer, which is also consistent with T_R values in the southwestern United States (Figs. 7b,c). This recurrence also continues for a second year, with significant autocorrelation values at lags up to 24 months centered on late summer/early fall.

Soil moisture reemergence is apparent in the cross correlation of the DJF (Fig. 8d), MAM (Fig. 8e), JJA (Fig. 8f), or SON (Fig. 8g) root zone soil moisture

anomaly with soil moisture anomalies at all lead/lags and depths. DJF and MAM root zone anomalies appear to descend below 1-m depth over a period of several months, reminiscent of Fig. 1. JJA (Fig. 8f) and SON (Fig. 8g) root zone soil anomalies also descend but not as deeply. DJF and MAM root zone soil moisture anomalies seem mostly correlated to future anomalies rather than to past anomalies, whereas JJA and SON root zone anomalies are significantly correlated to past anomalies as well. These panels all show an apparent reemergence signal in which the secondary autocorrelation function maximum (Fig. 8a) occurs when higher deep layer soil moisture memory reaches the surface from below.
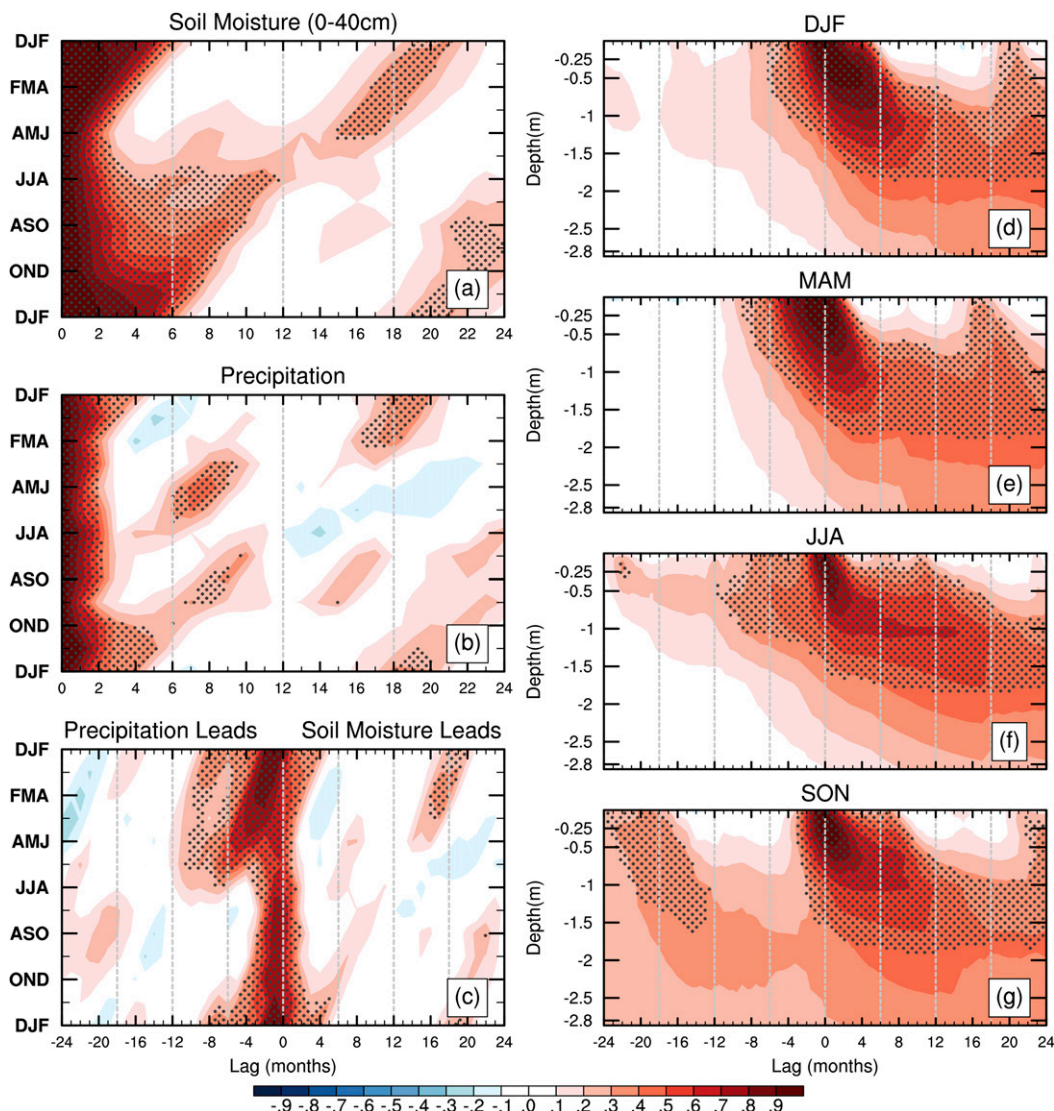
FIG. 8. Soil moisture statistics for the SW time series in the CLM dataset, for the years 1950–2010. Annual cycle of the autocorrelation function of (a) root zone soil moisture anomalies and (b) precipitation anomalies; (c) annual cycle of precipitation–root zone soil moisture cross correlation. In (c), positive lags refer to precipitation lagging soil moisture (i.e., soil moisture leading precipitation) and negative lags refer to precipitation leading soil moisture. For example, the location (4, DJF) indicates the correlation of DJF root zone soil moisture anomaly with the precipitation anomaly the following AMJ (i.e., 4 months later), while the location (−6, MJJ) indicates the correlation of MJJ root zone soil moisture anomaly with the precipitation anomaly the previous NDJ (i.e., 6 months earlier). (d)–(g) Cross correlation between the root zone soil moisture anomaly [in (d) DJF, (e) MAM, (f) JJA, and (g) SON] and the soil moisture anomaly as a function of depth and lead/lags. For example, in the SON panel the location (5, −0.5) indicates the correlation of SON root zone soil moisture anomaly with the soil moisture anomaly at depth 0.5 m in the following year FMA season (i.e., 5 months later); the location (−5, −0.8) in the DJF panel indicates the correlation of DJF root zone soil moisture anomaly with the soil moisture anomaly at depth 0.8 m in the previous year's JAS season (i.e., 5 months earlier).

Precipitation has less memory than root zone soil moisture (Fig. 8b), except in spring, and generally leads soil moisture (Fig. 8c), both as expected. However, November–January (NDJ) precipitation is also highly correlated with root zone soil moisture anomalies throughout the following winter and spring, even more than precipitation during the intervening months. For example, May–July (MJJ) root zone soil moisture is slightly more correlated with precipitation six months earlier (NDJ) than it is one month earlier (AMJ). This
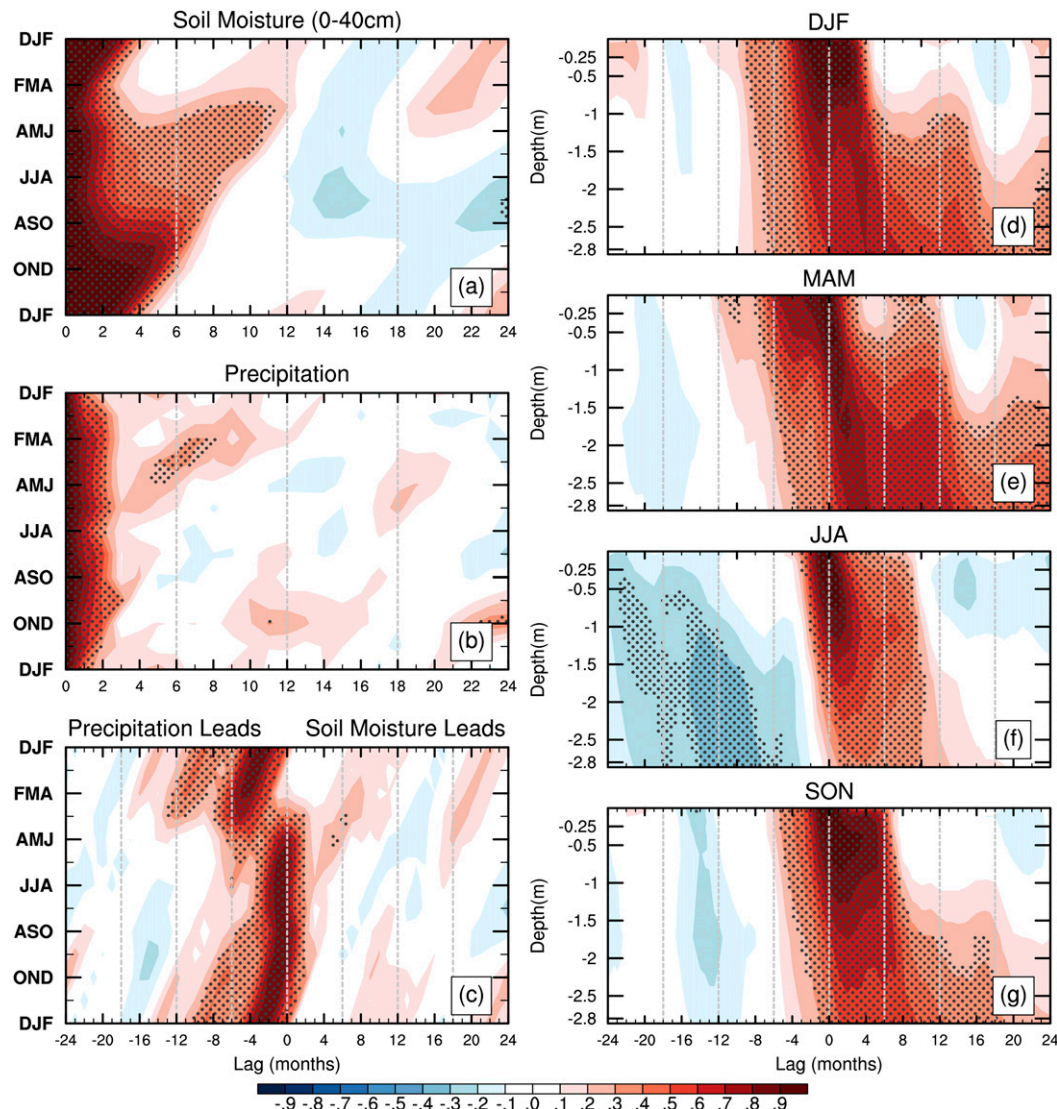
FIG. 9. As in Fig. 8, but for the GP time series.

could be consistent with NDJ precipitation forcing a soil moisture anomaly that persists and/or reemerges in late spring. Also, at some times when precipitation and root zone soil moisture recurrences appear to coincide, the cross-correlation function suggests that soil moisture leads precipitation (cf. maxima in Figs. 8a–c).

In the Great Plains (Fig. 9), soil moisture reemergence appears to occur in springtime. Higher soil moisture autocorrelation values at longer lags are fixed to the early-to-middle spring season (Fig. 9a), with a secondary maximum extending diagonally from about a 6-month lag starting in JAS to about a 12-month lag starting in MAM. The vertical correlation structure again shows apparent descent of soil moisture anomalies, reaching a greater depth than for the SW possibly because GP soil

conditions are comparatively more moist (Kumar et al. 2016). Springtime root zone soil moisture anomalies that recur the following year in early spring (Fig. 9a) appear driven by reemergence (Fig. 9e). Some signs of springtime reemergence also seem present for prior wintertime anomalies (Fig. 9d), but they do not quite reach the surface. There may also be a second-year reemergence centered in winter (cf. Figs. 9d and 9e to the recurrence at lags of 20–24 months in Fig. 9a). In contrast, there is significant 2-yr anticorrelation for summertime (JJA) soil moisture anomalies, also extending to deeper depth (Fig. 9f), which could be consistent with ENSO forcing (Yang et al. 2007). Note also that the weak precipitation recurrence seen between spring months and JJA (Fig. 9b) does not match the root zone soil moisture

recurrence ([Fig. 9a](#)). Moreover, while winter/early spring root zone soil moisture anomalies are not strongly correlated with the previous month's precipitation, they are correlated with precipitation from the previous fall [e.g., October–December (OND); [Fig. 9c](#)]. This relationship is consistent with the longer root zone memory seen at that time of the year ([Figs. 9a and 9g](#)) and also with recurrence from the previous spring (e.g., MAM; [Fig. 9c](#)), consistent with reemergence of the previous spring's soil moisture anomalies in [Fig. 9e](#).

Analysis for the Great Basin (Fig. S5) yields broadly similar features, but the GB time series has much longer soil moisture memory (~12 months) from late fall through early spring months than during the summer (~4 months), even as its precipitation has generally less memory than the SW and GP regions. The reemergence signal appears in the longer memory season (e.g., DJF and SON). This longer memory might be related to snow and soil freezing processes; however, data uncertainty due to poorly resolved topography in the CLM could also be an issue (Lawrence et al. 2019, manuscript submitted to *J. Adv. Model. Earth Syst.*).

c. Sensitivity to dataset

1) OTHER LDAS DATASETS

Sensitivity of these results to the LSM used was assessed by repeating the above analyses across the different LDAS products (CLM, VIC-highres, Noah, Mosaic, GLEAM, SMERGE, and MERRA-2) over the common 1980–2010 period. The resulting T_R maps (Fig. S4) show recurrence patterns that while broadly consistent have some fairly obvious quantitative differences.

The root zone soil moisture autocorrelation functions of the SW time series for all LDAS datasets and their ensemble mean, for the years 1980–2010, are compared in [Fig. 10](#). Also shown is the VIC-highres results for 1950–2010, which compares very well with the CLM for that period ([Fig. 8a](#)). The overall details, in particular recurrence magnitudes and time scales, are quite consistent between the two time periods in the VIC-highres, and across all LDAS datasets and the ensemble mean for 1980–2010. Soil moisture anomalies appear to reemerge during late summer from prior anomalies more than a year in advance. For example, DJF (AMJ) anomalies have a secondary maximum 20 (16) months later, during August–October (ASO). As in [Fig. 8](#), reemergence appears to occur in two successive summer seasons: SON soil moisture anomalies reemerge 8 months later, and again 22–24 months later.

The results for the GP time series ([Fig. 11](#)) are qualitatively similar across the datasets but have less quantitative agreement than in [Fig. 10](#). Greater differences

also exist between the post-1980 period and the full period in both the VIC-highres and CLM ([Fig. 9a](#)) and VIC-highres. The ensemble mean shows a stronger reemergence signal than the individual LDAS datasets, although all show significant recurrence during Fall; for example, February–April (FMA) soil moisture anomalies recur 8 months later (in OND), whereas AMJ soil moisture anomalies recur about 5–6 months later. Analysis of the GB time series (Fig. S6) shows even more discrepancies across the datasets, although most of the LDAS datasets have generally longer root zone soil moisture memory starting from the late fall through early spring months.

2) COMPARISON TO IN SITU DATA

Finally, we compare to the limited in situ records. [Figure 12](#) shows the Illinois root zone soil moisture autocorrelation function for the ICN and LDAS datasets. All show reemergence signals in their autocorrelation functions, but they appear to agree less well than in [Fig. 11](#), perhaps because of the smaller area or shorter data period. In fact, Noah shows significant negative autocorrelations, although SMERGE, which uses the Noah model to assimilate remote sensing–based surface soil moisture observations, does not. Still, most of the LDAS datasets agree better with each other than they do with the ICN. These differences are obviously concerning and could stem from deficiencies of the LDAS datasets (e.g., [Dirmeyer et al. 2016](#)), at least in the Illinois region ([Xia et al. 2014](#)). However, issues such as the scale mismatch between climate model grids and local ICN observations, the limited spatial and temporal sampling of the ICN dataset itself, and spatial heterogeneity in soil characteristics could also be impacting our correlation analysis. To test this possibility, we resampled the VIC-highres dataset using the days and 1/16° grid boxes that best corresponded to the available ICN data (no more than 18 locations and one to a few instantaneous samples per month), and then took the average over all the subsampled data to create the "VIC-highres-subsample" Illinois monthly time series. This produced a much better match to the ICN than did the original monthly mean data: the ICN and VIC-highres-subsample time series are notably better correlated, especially in the cold season (see [appendix A](#)), and extrema within the autocorrelation functions based on the VIC subsampled data and ICN ([Fig. 12](#)) also have considerably better correspondence. Additionally, the autocorrelation function and associated reemergence show substantial variation across all the individual ICN stations (Fig. S7), more often showing a stronger reemergence signal in the southern Illinois sites. Similar issues impact evaluation of soil moisture reemergence in
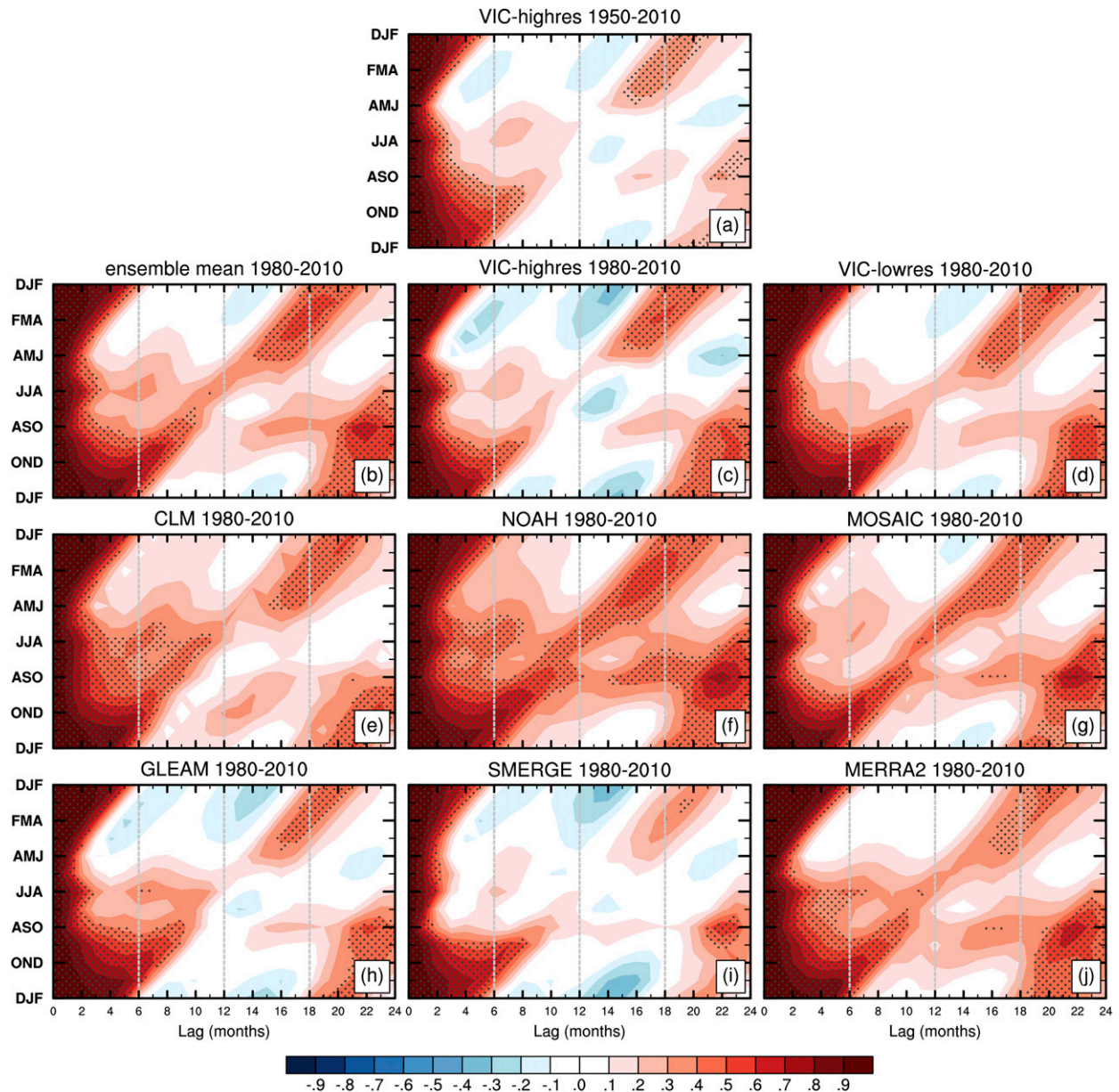
FIG. 10. Annual cycle of root zone soil moisture anomaly autocorrelation function for the SW time series, in LDAS datasets. All figures represent results from 1980 to 2010, except for the top row center, which shows 1950–2010. Results for the ensemble mean for 1980–2010 are shown in the second row left corner.

the vertical cross sections (see Figs. S8 and S9). Given all of these considerations, it appears to be difficult to draw firm conclusions from the ICN results, at least quantitatively.

Figure 13 shows the root zone soil moisture autocorrelation functions at six other sites with relatively long records and with soil moisture measurements down to a depth of at least 40 cm. These show that autocorrelation

structures with significant differences from simple exponential decay are prevalent across observation sites throughout the United States. For example, three (Mandan, Long Valley, and Reynold's Creek) out of six sites show robust reemergence signals. The remaining three sites also show reemergence signals, but they are weak and not statistically significant; two sites have some negative correlations originating in winter that

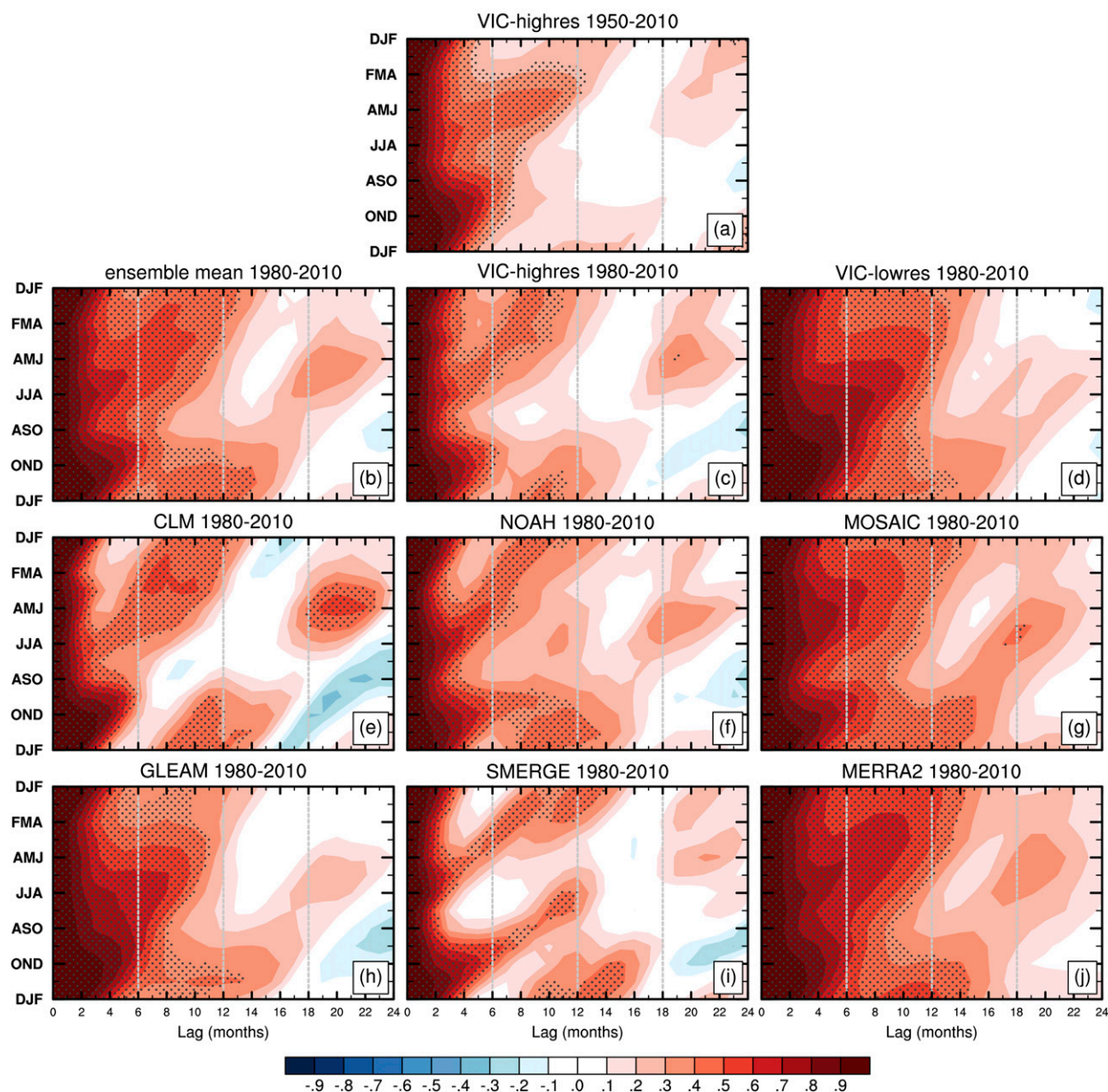## GREAT PLAINS Rootzone Soil Moisture

FIG. 11. As in Fig. 10, but showing the annual cycle of root zone soil moisture anomaly autocorrelation function for the GP time series, in the LDAS datasets. All figures represent results from 1980 to 2010, except for the top row center, which shows 1950–2010. Results for the ensemble mean for 1980–2010 are shown in the second row left corner.

might be due to precipitation forcing and/or data uncertainty due to snow cover (Quiring et al. 2016). A comparison of 13 years of LDAS data at Reynold's Creek site shows qualitatively similar results (e.g., the reemergence signal in the summer and fall seasons; Fig. S10). Results for the different sites seem to somewhat correspond to the LDAS results discussed above, but again the limited sample sizes and localized nature

of the in situ measurements make a more detailed assessment difficult.

d. Sensitivity to precipitation variability

One obvious issue raised by the precipitation correlations in section 4b is whether root zone soil moisture recurrence truly represents reemergence and other land surface processes, or whether it is largely driven by

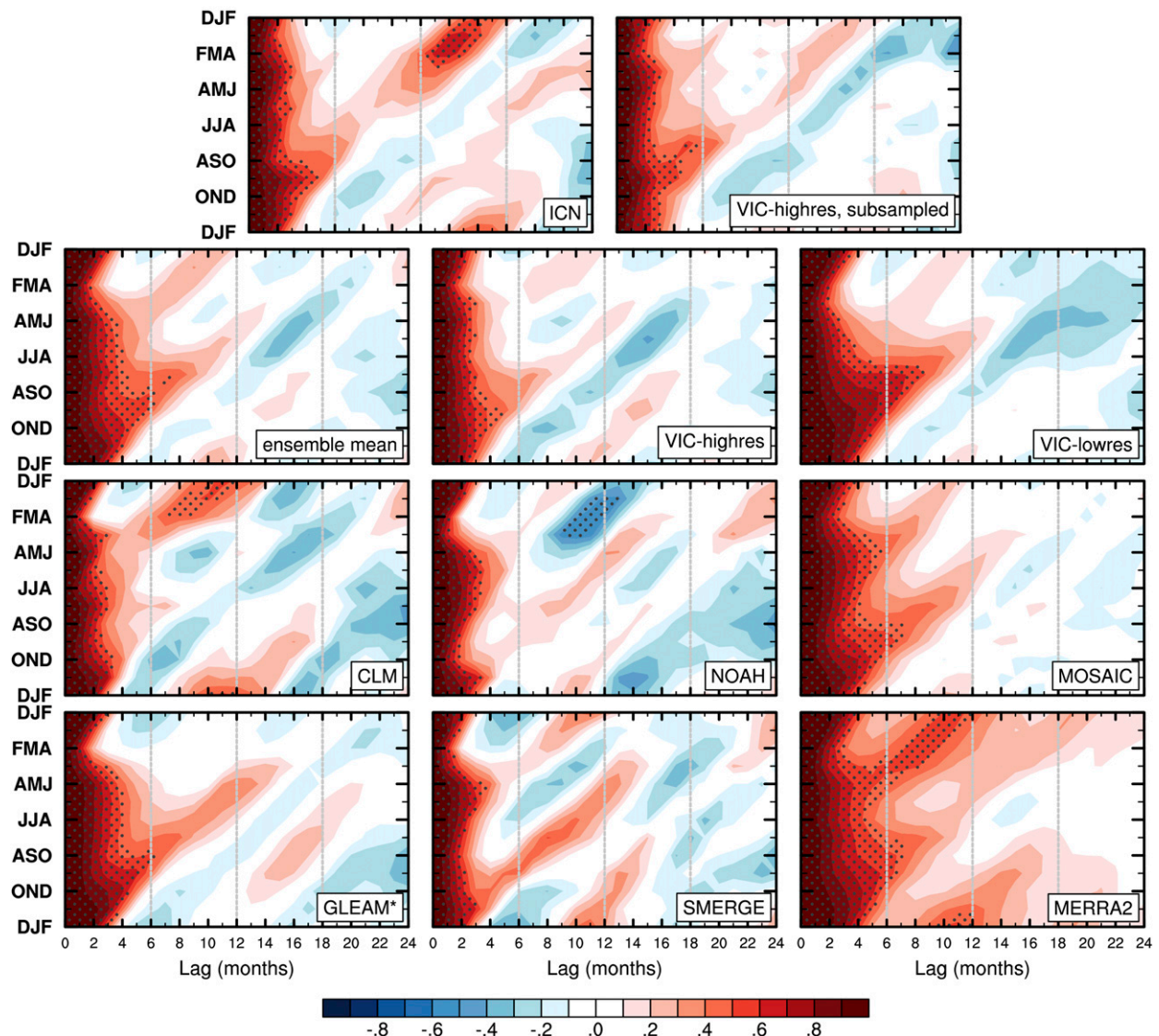## ILLINOIS 1985-2004 Rootzone Soil Moisture

FIG. 12. Annual cycle of root zone soil moisture autocorrelation function for Illinois from all soil moisture dataset (cf. Table 1). Ensemble mean results include all soil datasets shown here except for the subsampled version of the VIC-highres.

recurring atmospheric forcing (e.g., precipitation; Figs. 8b and 9b). Similarly, significant negative soil moisture autocorrelation could represent atmospheric rather than land effects, either due to oceanic forcing or to sampling of random weather events. On the other hand, while the observed precipitation recurrence could be due to climate forcing, Figs. 8c and 9c suggest it could also result from land feedbacks—for example, from atmospheric coupling to a root zone layer responding to soil moisture reemergence. To initially explore these issues, we compared the VIC-lowres soil moisture dataset to two corresponding VIC-lowres datasets used in Livneh and Hoerling (2016), which

were created using observed atmospheric forcing as before except 1) the precipitation variability was removed (i.e., precipitation was fixed to its annual cycle; "precip climo"), or 2) the temperature variability was removed (i.e., temperature was fixed to its annual cycle; "temp climo"). We also compared to the CPC soil moisture dataset that, while also forced with observations, had no vertical structure in its LSM. Since the CPC dataset represents a 1.6-m-thick surface layer, we compared to the top 1 m (rather than top 0.4 m) soil moisture from the VIC-lowres datasets; this mainly tended to slightly lengthen overall memory and thereby weaken reemergence strength relative to results
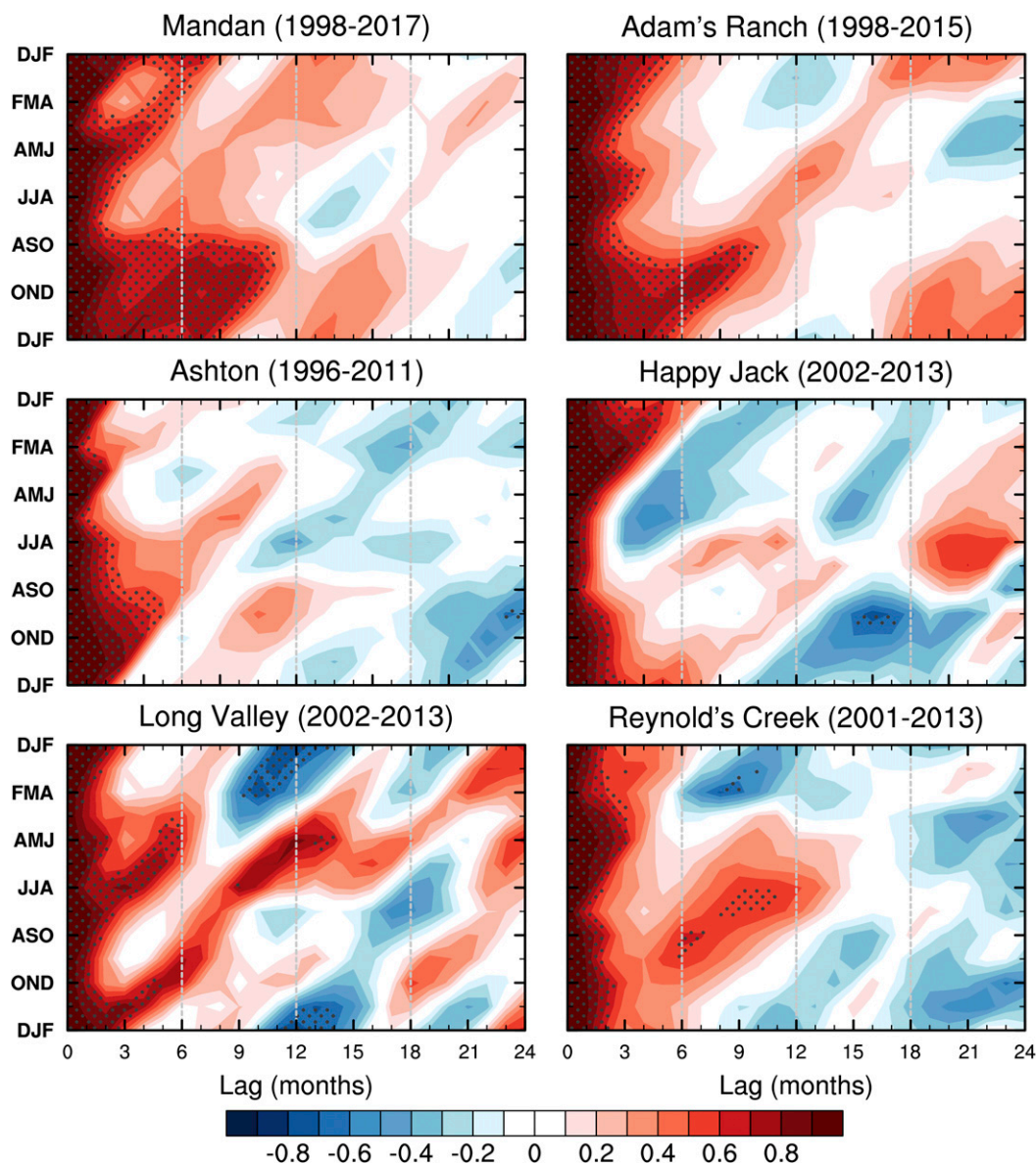
FIG. 13. Annual cycle of root zone soil moisture autocorrelation for selected in situ sites (see text for more details, and Fig. A2 for site locations).

using the top 0.4-m layer but had no other qualitative impact.

Figure 14 shows the SW autocorrelation function in the four different datasets. Removing observed precipitation variability yielded a reduction of the correlation between fall and subsequent spring soil moisture, which could be due to removing persistent cool season ENSO forcing in the Southwest (note in Fig. 8b that the fall/winter precipitation autocorrelation is significant for lags of up to 5 months). Still, some soil moisture recurrence remains, suggesting that it may not only be forced by precipitation. Additionally, for lags greater

than about 6 months, recurrence was not reduced; instead, it appears that the precipitation variability may even have obscured a stronger summertime reemergence signal. Removing temperature variability, in comparison, had minimal effect. It is interesting to note that even the very simple CPC hydrology model showed a similar recurrence pattern in the second year. This supports climate forcing (precipitation and evaporative demand) as a key driver compared with soil moisture vertical discretization in the model, although it does not rule out possible land–atmosphere feedbacks related to reemergence.
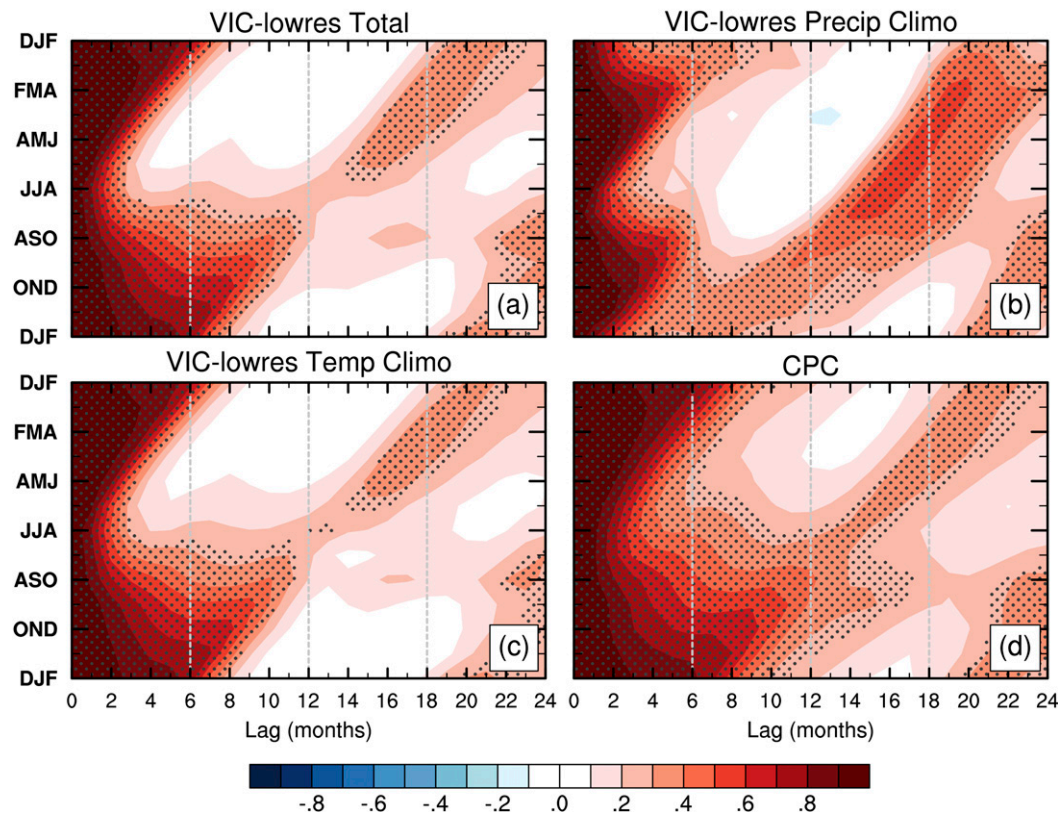
FIG. 14. Annual cycle of top 1-m soil moisture autocorrelation for the SW time series, from different VIC-lowres datasets based on (a) observed forcing (cf. Fig. 11), (b) observed temperature and climatological precipitation forcing ("precip climo"), and (c) climatological temperature and observed precipitation forcing ("temp climo"), for the years 1950–2010. (d) The corresponding analysis applied to the same region and period in the CPC ("leaky bucket") dataset. Note that unlike previous figures, these results are for the 0–1-m soil layer, except for CPC, which represents 0–1.6 m.

Figure 15 shows the same analysis for the GP time series. Here we see no reduction in autocorrelation values when precipitation variability is removed; in fact, since anomaly recurrence at longer lags is amplified, it again appears that precipitation variability may have partly obscured a stronger reemergence signal that also clearly extended to a second successive spring. Moreover, the recurrence signal is notably weaker in the CPC dataset, especially in the second year, further supporting the importance of GP reemergence. For the GB time series, in contrast, precipitation variability appears to drive the bulk of the persistence and reemergence signals except for a weaker signal during the warm season (see Fig. S11). However, given the poorer agreement across the LDAS datasets for the arid GB region, confidence in this result is low.

5. Concluding remarks

In this study, we aimed to investigate mechanisms of long-term soil moisture memory, using a statistical (i.e.,

correlations-based) analysis of in situ observations and LDAS datasets over North America. We defined and identified for the first time a "soil moisture reemergence" process, which could lead to improved understanding of long-term drought and pluvial processes and also be a source of soil moisture predictability on seasonal to interannual (or possibly longer) time scales.

In the extratropical oceans, the memory time scale of upper ocean thermal anomalies is on the order of a few seasons. Yet, both observational and modeling studies have shown that extratropical sea surface temperature anomalies tend to recur from one winter to the next, even as they do not typically persist during the intervening summer, due to a process Alexander and Deser (1995) called reemergence (Alexander and Deser 1995; Alexander et al. 1999; Namias and Born 1970). In the ocean, reemergence occurs because wintertime thermal anomalies are well mixed downward throughout the deep winter mixed layer, become decoupled from the surface when the mixed layer shallows in the
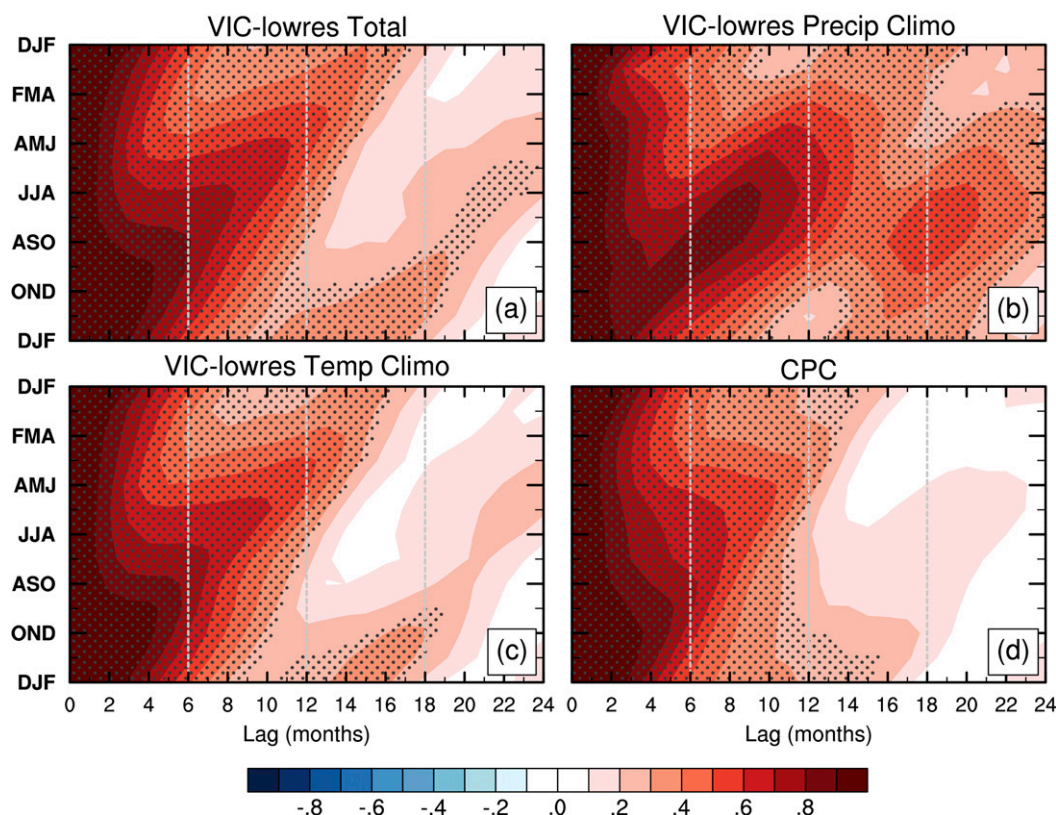
1950-2010 GREAT PLAINS Soil Moisture(0-1m)

FIG. 15. As in Fig. 14, but showing the annual cycle of top 1-m soil moisture autocorrelation for the GP time series, from different VIC-lowres datasets based on (a) observed forcing (cf. Fig. 12), (b) observed temperature and climatological precipitation forcing ("precip climo"), and (c) climatological temperature and observed precipitation forcing ("temp climo"), for the years 1950–2010. (d) The corresponding analysis applied to the same region and period in the CPC ("leaky bucket") dataset.

summer, and are re-entrained into the mixed layer as it deepens the following winter. Soil moisture reemergence is an analogous process because it too represents strong seasonal modulation in the coupling between a surface layer with short memory and a deeper layer with longer memory, wherein 1) in the first season, surface forcing creates an anomaly that propagates into the deep layer; 2) in the next season, the layers are effectively decoupled so that the anomaly decays at the surface but persists in the deep layer; and 3) eventually, coupling is reestablished, driving the surface back toward its prior anomaly. In the ocean, this process has a clear signature in the seasonally varying autocorrelation function: a secondary maximum tilted diagonally so that it is tied to a fixed season rather than a fixed lag (Newman et al. 2003). That a similar feature also appears in the root zone soil moisture autocorrelation function (e.g., Figs. 2a, 8a, and 9a) is evidence for a similar reemergence process for soil moisture.

Nevertheless, it is important to clearly distinguish between our results and our interpretation of them,

since ultimately we believe this study raises more questions than it answers. Primarily using long-term (60 yr) LSM-based (LDAS) soil moisture datasets, we have found statistically significant recurrence of root zone soil moisture seasonal anomalies for lags as long as 2 years, which is considerably longer than the generally accepted memory time scale of root zone anomalies. This recurrence is usually strongly related to the seasonal cycle, so it is often apparent only during isolated seasons and not year-round. These results immediately suggest that root zone soil moisture is likely predictable on time scales measured in seasons and maybe even years, not just months.

We interpret these results as evidence of a soil moisture reemergence process, not only due to the diagonal features in the autocorrelation function, but also because at the same time there appears to be propagation of anomalies to the deeper soil in some seasons with the later reemergence of these anomalies. This is our interpretation of the vertical cross-section plots (Figs. 8d–g

and 9d–g) where the recurrence of root zone soil moisture anomalies (corresponding to Figs. 8a and 9a) was better correlated with prior deep layer anomalies than to either the root zone anomalies of the previous season or to atmospheric forcing (i.e., precipitation). Experiments with the lower-resolution version of the VIC model also suggest that atmospheric variations alone cannot explain the observed recurrence.

We hypothesized two possible mechanisms: 1) the demand-driven hypothesis and 2) the anomaly propagation hypothesis. Data presented here are consistent with both hypotheses. Additional observations and numerical experiments are needed to quantify their relative contributions. For example, data from the multidecadal drought period may clarify the role of the anomaly propagation hypothesis. Similarly, numerical experiments with and without deep layer soil moisture memory and its impacts on soil moisture anomalies during the summer may clarify the role of the demand-driven hypothesis.

One of the underappreciated implications of oceanic reemergence is that extratropical decadal variability and predictability may have pronounced seasonality. That is, a decadal signal may only exist in one particular season, not necessarily year-round. This may also be true for predictability stemming from soil moisture reemergence. Also, note that much of the PDO's variability results from reemergence acting to redden the ENSO signal in the North Pacific (Newman et al. 2016). It is an interesting question whether soil moisture reemergence might act similarly to redden the ENSO signal over land, and if so whether this is why, as previously suggested by Newman et al. (2003), there is an apparent pronounced PDO signal in North American drought (Barlow et al. 2001) and in climate proxies such as tree rings (Biondi et al. 2001; D'Arrigo and Wilson 2006).

In summary, while much of the evidence put forth here in support of soil moisture reemergence is compelling, it is also largely circumstantial due primarily to the lack of direct observations needed, ICN data notwithstanding—hence the caveat "potential reemergence" in the paper title. Our statistical analysis suggests a new and interesting physical process, but multiple questions remain: the extent to which the process exists, how consistent it is with our physical hypotheses, and how quantitatively important it is to the land–atmosphere climate system. Since our analysis was limited to relatively shorter in situ and only somewhat longer model-based datasets, its considerable quantitative uncertainty could reflect sampling issues, meaning that longer data records (which may be unavailable) are required to isolate reemergence from weather and climate variability and land–atmosphere coupling. However, we also cannot exclude the possibility that

reemergence acts quite differently in the current generation of LSMs than it does in nature. Many potentially interacting but largely undetermined factors can also affect soil moisture reemergence, including precipitation variability and persistence, land–atmosphere coupling, and the distribution of soil types both horizontally and vertically. LSM representation of reemergence could be additionally complicated by factors including (but not limited to) vertical discretization and soil moisture model parameterizations, and by how well they represent seasonal and regional variations of all the above variables. For example, Livneh et al. (2015a) found that the same LSM produced different portrayals of long memory processes like drought when driven with different underlying soil survey data. In particular a rigorous sensitivity analysis of the role of model parameter settings and layer discretization would be needed to assert a more quantitative measure of reemergence beyond the qualitative assessment presented here. The effects of land use land cover type, interactive vegetation phenology, and hydraulic redistribution by the plant root system could also be relevant. Finally, while we ruled out significant impacts on our results by a seasonally varying linear trend, more complex effects of anthropogenic change are still possible. Addressing all of these questions will require additional analysis of related hydrological observations and a systematic experimental framework ranging from simple multivariate autoregressive models to stand-alone land models and complex coupled climate models.

APPENDIX A

Station Data Processing

a. Processing of ICN data

At each of 18 sites throughout Illinois (see Fig. A1), ICN observations were taken at least twice per month during the growing season, which we averaged together, and once per month otherwise for the years 1983–2004 (although irregular sampling meant that some months were skipped at some stations in some years). These measurements were then taken to represent the monthly averages at each site. Each soil layer was processed separately; if a layer was missing it was filled in with
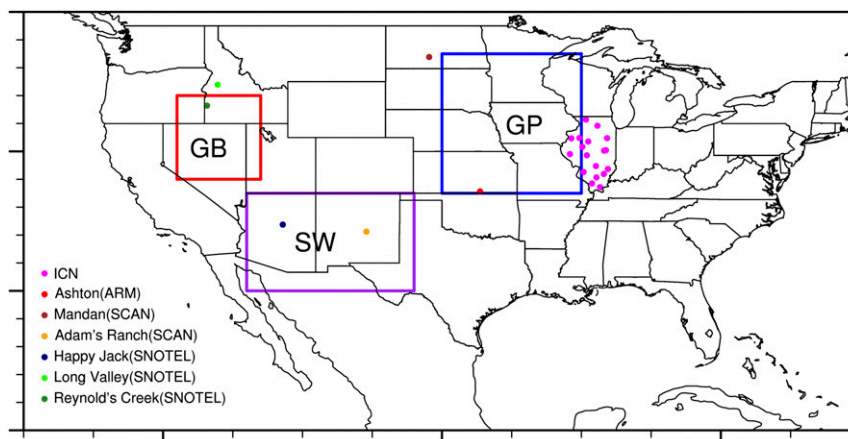
Fig. A1. Locations of station data and the boundaries for the three regional indexes used in this study.

weighted linear interpolation, but if more than one layer was missing from the root zone and two layers were missing from the deep layer the site was recorded as missing for that month. Then, we determined the root zone (0–0.4 m) soil moisture at each site for each month, and subsequently averaged the monthly root zone soil moisture across the available sites each month to represent the Illinois average root zone soil moisture total field. ICN soil moisture data were available from 1983 to 2004 for most of the stations, but the first two years were excluded due to outliers that were more than four standard deviations away from the mean of all data (Xia et al. 2014).

Figure A2 shows the Illinois-mean seasonal anomaly correlations of ICN soil moisture data with the LDAS datasets for the root zone (0–0.4 m). All LDAS anomalies are generally better correlated with ICN anomalies during the growing season (spring and summer) than the
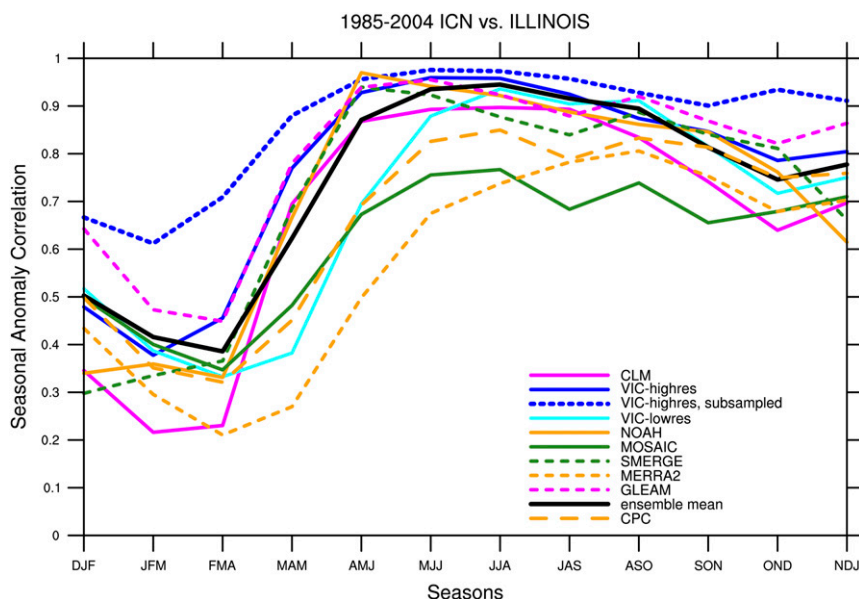

Fig. A2. Correlation of ICN mean root zone soil moisture anomaly with corresponding anomaly from each soil moisture dataset averaged within Illinois, as a function of season for the years 1985–2004. Note that the CPC dataset represents soil moisture in the 0–1.6-m layer. Ensemble mean results here include all datasets except CPC, and the subsampled version of the VIC-highres. Three instances of VIC are included to illustrate differences in model scale configuration, as well as the importance of subsampling daily model outputs on the sampling dates and location of the ICN stations.

winter seasons, as was earlier found by Xia et al. (2014). For example, VIC-highres shows an anomaly correlation of ~0.9 from AMJ through ASO seasons but drops below 0.5 for DJF through FMA seasons. VIC-highres anomalies generally correspond better with the ICN compared to other LDAS datasets for most of the year.

To investigate the issue of sparse and irregular temporal frequency of ICN observations, we subsampled VIC-highres soil moisture data to the nearest location (1/16° grid box) and day of observation at the respective stations before taking the area and monthly average; the number of stations each month varied consistent with ICN data availability. This time series, called the VIC-highres-subsample, has notably higher correlations with the ICN monthly time series, especially throughout most of the cold season (Fig. A2). This suggests that the effect of sampling (primarily temporal; not shown) at the ICN sites is nontrivial, and likewise that LDAS datasets (at least the VIC-highres, at these locations, for 3-month averages) may better represent in situ data than the comparison in Xia et al. (2014) suggests. Spatial heterogeneity in soil characteristics may likewise be an issue. If all this is the case, it may even be that the full monthly averaged Illinois-mean VIC-highres time series is as good or even better a representation of soil moisture over the 1982–2015 period than the ICN time series.

b. Processing of other station data

We also examined raw station data from sites other than the ICN. Data were downloaded from the ISMN website (http://ismn.geo.tuwien.ac.at), selected in or near the predefined regions (GP, SW, and GB). We found six stations (2 from SCAN, 3 from SNOTEL, and 1 from ARM) that all have a record length of at least 12 years and soil moisture observations down to at least 0.5 m. Some other stations or networks that also have relatively long records contained too much missing data (e.g., the SNOTEL station SILVIES) or were systematically missing certain months of the year (e.g., the IOWA network) to make for a representative determination of the seasonal cycle of the autocorrelation function.

APPENDIX B

Autocorrelation Function and Significance Testing

The autocorrelation function was determined separately for each month by correlating the soil moisture anomalies at time = 0 with values at lags and leads ranging from −24 months to +24 months. This was done both for the same soil layer [autocorrelation (AC)] and between two different soil layers [cross correlation

(CC)]. Let us suppose that $\prod_{y=1,m=1,l=1}^{y=n,m=12,l=11} X_{y,m,l}$ is the seasonal anomalies time series where subscript y represents year (1–n), m represents season (1–12), and l represents soil layer; then the correlation functions are given as below:

$$\mathrm{AC}_{m,l,\delta} = \mathrm{correl}\left(\prod_{y=1}^{n} X_{y,m,l}, \prod_{y=1}^{n} X_{y,m+\delta,l}\right), \quad (B1)$$

$$\mathrm{CC}_{m,l_1 l_2,\delta} = \mathrm{correl}\left(\prod_{y=1}^{n} X_{y,m,l_1}, \prod_{y=1}^{n} X_{y,m+\delta,l_2}\right), \quad (B2)$$

where $\mathrm{AC}_{m,l,\delta}$ is autocorrelations for season m, layer l, and at lead/lag δ, which ranges from −24 to 24. The term $\mathrm{CC}_{m,l_1 l_2,\delta}$ is the cross correlation between layer l_1 and l_2 for season m and lead/lag δ; Correl is the linear correlation coefficient between the two series. For $m + \delta > 12$, $X_{y,m+\delta,l} = X_{y+1,m+\delta-12,l}$, and $m + \delta < 0$, $X_{y,m+\delta,l} = X_{y-1,m+\delta+12,l}$. We determined the t statistic for the regression coefficient and converted the t statistic into the statistical probabilities (p value). Thus, every year contributes one sample in the given time series, (e.g., $\prod_{y=1}^{n} X_{y,m,l}$). We determined degrees of freedom by accounting for serial autocorrelation in the time series and accordingly reducing the effective sample size using the NCL function equiv_sample_size (NCL 2018). For example, the number of degrees of freedom for 20 years of Illinois seasonal anomalies was 16. We label AC or CC values with a p value ≤ 0.05 for two-tailed test as statistically significant.

Additionally, for every significant AC and CC value we tested whether it represented a linear relationship, by finding the linear, quadratic, and cubic least squares fits to the data used to determine the correlation value (examples are shown in Fig. S12). The Bayesian information criterion (BIC) test was then applied in each case to select which of these three curves was the best model of the data scatterplot. We found that in 94% of the values tested, the linear fit was the best.

REFERENCES

Alexander, M., and C. Deser, 1995: A mechanism for the recurrence of wintertime midlatitude SST anomalies. *J. Phys. Oceanogr.*, **25**, 122–137, https://doi.org/10.1175/1520-0485(1995)025<0122:AMFTRO>2.0.CO;2.

——, ——, and M. S. Timlin, 1999: The reemergence of SST anomalies in the North Pacific Ocean. *J. Climate*, **12**, 2419–2433, https://doi.org/10.1175/1520-0442(1999)012<2419:TROSAI>2.0.CO;2.

Amenu, G. G., and P. Kumar, 2008: A model for hydraulic redistribution incorporating coupled soil–root moisture transport. *Hydrol. Earth Syst. Sci.*, **12**, 55–74, https://doi.org/10.5194/hess-12-55-2008.

——, ——, and X.-Z. Liang, 2005: Interannual variability of deep-layer hydrologic memory and mechanisms of its influence on surface energy fluxes. *J. Climate*, **18**, 5024–5045, https://doi.org/10.1175/JCLI3590.1.

Asner, G. P., P. G. Brodrick, C. B. Anderson, N. Vaughn, D. E. Knapp, and R. E. Martin, 2016: Progressive forest canopy water loss during the 2012–2015 California drought. *Proc. Natl. Acad. Sci. USA*, **113**, E249–E255, https://doi.org/10.1073/pnas.1523397113.

Ault, T. R., and Coauthors, 2013: The continuum of hydroclimate variability in western North America during the Last Millennium. *J. Climate*, **26**, 5863–5878, https://doi.org/10.1175/JCLI-D-11-00732.1.

——, and Coauthors, 2018: A robust null hypothesis for the potential causes of megadrought in western North America. *J. Climate*, **31**, 3–24, https://doi.org/10.1175/JCLI-D-17-0154.1.

Barlow, M., S. Nigam, and E. H. Berbery, 2001: ENSO, Pacific decadal variability, and U.S. summertime precipitation, drought, and stream flow. *J. Climate*, **14**, 2105–2128, https://doi.org/10.1175/1520-0442(2001)014<2105:EPDVAU>2.0.CO;2.

Bellucci, A., and Coauthors, 2015: Advancements in decadal climate predictability: The role of nonoceanic drivers. *Rev. Geophys.*, **53**, 165–202, https://doi.org/10.1002/2014RG000473.

Bierkens, M. F. P., and B. J. J. M. van den Hurk, 2007: Groundwater convergence as a possible mechanism for multi-year persistence in rainfall. *Geophys. Res. Lett.*, **34**, L02402, https://doi.org/10.1029/2006GL028396.

Biondi, F., A. Gershunov, and D. R. Cayan, 2001: North Pacific decadal climate variability since 1661. *J. Climate*, **14**, 5–10, https://doi.org/10.1175/1520-0442(2001)014<0005:NPDCVS>2.0.CO;2.

Bonan, G. B., K. W. Oleson, M. Vertenstein, S. Levis, X. Zeng, Y. Dai, R. E. Dickinson, and Z. Yang, 2002: The land surface climatology of the Community Land Model coupled to the NCAR Community Climate Model. *J. Climate*, **15**, 3123–3149, https://doi.org/10.1175/1520-0442(2002)015<3123:TLSCOT>2.0.CO;2.

Bond, D., 2005: Soil Water and Temperature System (SWATS) handbook. U.S. Department of Energy Tech. Rep. ARM TR-063, 24 pp.

Chen, F., and Coauthors, 2014: Modeling seasonal snowpack evolution in the complex terrain and forested Colorado Headwaters region: A model intercomparison study. *J. Geophys. Res. Atmos.*, **119**, 13 795–13 819, https://doi.org/10.1002/2014JD022167.

Chen, M., P. Xie, J. E. Janowiak, and P. A. Arkin, 2002: Global land precipitation: A 50-yr monthly analysis based on gauge observations. *J. Hydrometeor.*, **3**, 249–266, https://doi.org/10.1175/1525-7541(2002)003<0249:GLPAYM>2.0.CO;2.

——, W. Shi, P. P. Xie, V. B. S. Silva, V. E. Kousky, R. W. Higgins, and J. E. Janowiak, 2008: Assessing objective techniques for gauge-based analyses of global daily precipitation. *J. Geophys. Res.*, **113**, D04110, https://doi.org/10.1029/2007JD009132.

Cheng, L. Y., M. Hoerling, A. AghaKouchak, B. Livneh, X. W. Quan, and J. Eischeid, 2016: How has human-induced climate change affected California drought risk? *J. Climate*, **29**, 111–120, https://doi.org/10.1175/JCLI-D-15-0260.1.

Chikamoto, Y., A. Timmermann, S. Stevenson, P. DiNezio, and S. Langford, 2015: Decadal predictability of soil water, vegetation, and wildfire frequency over North America. *Climate Dyn.*, **45**, 2213–2235, https://doi.org/10.1007/s00382-015-2469-5.

Coats, S., J. E. Smerdon, K. B. Karnauskas, and R. Seager, 2016: The improbable but unexceptional occurrence of megadrought clustering in the American West during the Medieval Climate Anomaly. *Environ. Res. Lett.*, **11**, 074025, https://doi.org/10.1088/1748-9326/11/7/074025.

Cole, J. E., J. T. Overpeck, and E. R. Cook, 2002: Multiyear La Niña events and persistent drought in the contiguous United States. *Geophys. Res. Lett.*, **29**, 1647, https://doi.org/10.1029/2001GL013561.

Cook, B. I., and Coauthors, 2016: North American megadroughts in the Common Era: Reconstructions and simulations. *Wiley Interdiscip. Rev.: Climate Change*, **7**, 411–432, https://doi.org/10.1002/wcc.394.

Cook, E. R., C. A. Woodhouse, C. M. Eakin, D. M. Meko, and D. W. Stahle, 2004: Long-term aridity changes in the western United States. *Science*, **306**, 1015–1018, https://doi.org/10.1126/science.1102586.

Crow, W., and K. Tobin, 2018: Smerge-Noah-CCI root zone soil moisture 0-40 cm L4 daily 0.125 × 0.125 degree V1.0. Goddard Earth Sciences Data and Information Services Center (GES DISC), accessed 15 October 2018, https://doi.org/10.5067/NRJWAMBMN6JD.

D'Arrigo, R., and R. Wilson, 2006: On the Asian expression of the PDO. *Int. J. Climatol.*, **26**, 1607–1617, https://doi.org/10.1002/joc.1326.

Delworth, T. L., and S. Manabe, 1988: The influence of potential evaporation on the variabilities of simulated soil wetness and climate. *J. Climate*, **1**, 523–547, https://doi.org/10.1175/1520-0442(1988)001<0523:TIOPEO>2.0.CO;2.

Deser, C., M. A. Alexander, and M. S. Timlin, 2003: Understanding the persistence of sea surface temperature anomalies in midlatitudes. *J. Climate*, **16**, 57–72, https://doi.org/10.1175/1520-0442(2003)016<0057:UTPOSS>2.0.CO;2.

Dirmeyer, P. A., and Coauthors, 2016: Confronting weather and climate models with observational data from soil moisture networks over the United States. *J. Hydrometeor.*, **17**, 1049–1067, https://doi.org/10.1175/JHM-D-15-0196.1.

Dorigo, W. A., and Coauthors, 2011: The International Soil Moisture Network: A data hosting facility for global in situ soil moisture measurements. *Hydrol. Earth Syst. Sci.*, **15**, 1675–1698, https://doi.org/10.5194/hess-15-1675-2011.

——, and Coauthors, 2013: Global automated quality control of in situ soil moisture data from the International Soil Moisture Network. *Vadose Zone J.*, **12**, vzj2012.0097, https://doi.org/10.2136/vzj2012.0097.

Ek, M. B., K. E. Mitchell, Y. Lin, E. Rogers, P. Grunmann, V. Koren, G. Gayno, and J. D. Tarpley, 2003: Implementation of Noah land surface model advances in the National Centers for Environmental Prediction operational mesoscale Eta model. *J. Geophys. Res.*, **108**, 8851, https://doi.org/10.1029/2002JD003296.

Entekhabi, D., I. Rodriguez-Iturbe, and F. Castelli, 1996: Mutual interaction of soil moisture state and atmospheric processes. *J. Hydrol.*, **184**, 3–17, https://doi.org/10.1016/0022-1694(95)02965-6.

Entin, J. K., A. Robock, K. Y. Vinnikov, S. E. Hollinger, S. Liu, and A. Namkhai, 2000: Temporal and spatial scales of observed soil moisture variations in the extratropics. *J. Geophys. Res.*, **105**, 11865–11877, https://doi.org/10.1029/2000JD900051.

Evans, J. P., X. H. Meng, and M. F. McCabe, 2017: Land surface albedo and vegetation feedbacks enhanced the millennium drought in south-east Australia. *Hydrol. Earth Syst. Sci.*, **21**, 409–422, https://doi.org/10.5194/hess-21-409-2017.

Fan, Y., and H. van den Dool, 2004: Climate Prediction Center global monthly soil moisture data set at 0.5° resolution for 1948

to present. *J. Geophys. Res.*, **109**, D10102, https://doi.org/10.1029/2003JD004345.

——— and G. Miguez-Macho, 2010: Potential groundwater contribution to Amazon evapotranspiration. *Hydrol. Earth Syst. Sci.*, **14**, 2039–2056, https://doi.org/10.5194/hess-14-2039-2010.

Gao, X. Y., Z. L. Huo, Z. Y. Qu, X. Xu, G. H. Huang, and T. S. Steenhuis, 2017: Modeling contribution of shallow groundwater to evapotranspiration and yield of maize in an arid area. *Sci. Rep.*, **7**, 43122, https://doi.org/10.1038/srep43122.

Gelaro, R., and Coauthors, 2017: The Modern-Era Retrospective Analysis for Research and Applications, version 2 (MERRA-2). *J. Climate*, **30**, 5419–5454, https://doi.org/10.1175/JCLI-D-16-0758.1.

Ghannam, K., T. Nakai, A. Paschalis, C. A. Oishi, A. Kotani, Y. Igarashi, T. Kumagai, and G. G. Katul, 2016: Persistence and memory timescales in root-zone soil moisture dynamics. *Water Resour. Res.*, **52**, 1427–1445, https://doi.org/10.1002/2015WR017983.

Goldsmith, G. R., 2013: Changing directions: The atmosphere–plant–soil continuum. *New Phytol.*, **199**, 4–6, https://doi.org/10.1111/nph.12332.

Green, W. H., and G. A. Ampt, 1911: Studies on soil physics. *J. Agric. Sci.*, **4**, 1–24, https://doi.org/10.1017/S0021859600001441.

Guo, Z. C., P. A. Dirmeyer, and T. DelSole, 2011: Land surface impacts on subseasonal and seasonal predictability. *Geophys. Res. Lett.*, **38**, L24812, https://doi.org/10.1029/2011GL049945.

Hasselmann, K., 1976: Stochastic climate models. Part I. Theory. *Tellus*, **28**, 473–485, https://doi.org/10.3402/tellusa.v28i6.11316.

Held, I. M., T. L. Delworth, J. Lu, K. L. Findell, and T. R. Knutson, 2005: Simulation of Sahel drought in the 20th and 21st centuries. *Proc. Natl. Acad. Sci. USA*, **102**, 17 891–17 896, https://doi.org/10.1073/pnas.0509057102.

Herweijer, C., R. Seager, E. R. Cook, and J. Emile-Geay, 2007: North American droughts of the last millennium from a gridded network of tree-ring data. *J. Climate*, **20**, 1353–1376, https://doi.org/10.1175/JCLI4042.1.

Hoerling, M., and A. Kumar, 2003: The perfect ocean for drought. *Science*, **299**, 691–694, https://doi.org/10.1126/science.1079053.

——, J. Eischeid, A. Kumar, R. Leung, A. Mariotti, K. Mo, S. Schubert, and R. Seager, 2014: Causes and predictability of the 2012 Great Plains drought. *Bull. Amer. Meteor. Soc.*, **95**, 269–282, https://doi.org/10.1175/BAMS-D-13-00055.1.

Hollinger, S. E., and S. A. Isard, 1994: A soil moisture climatology of Illinois. *J. Climate*, **7**, 822–833, https://doi.org/10.1175/1520-0442(1994)007<0822:ASMCOI>2.0.CO;2.

Howitt, R., D. MacEwan, J. Medellín-Azuara, J. Lund, and D. Sumner, 2015: Economic analysis of the 2015 drought for California agriculture. UC Davis Center for Watershed Sciences, 31 pp.

Huang, J., H. M. van den Dool, and K. P. Georgakakos, 1996: Analysis of model-calculated soil moisture over the United States (1931–1993) and applications to long-range temperature forecasts. *J. Climate*, **9**, 1350–1362, https://doi.org/10.1175/1520-0442(1996)009<1350:AOMCSM>2.0.CO;2.

Huete, A. R., and Coauthors, 2006: Amazon rainforests green-up with sunlight in dry season. *Geophys. Res. Lett.*, **33**, L06405, https://doi.org/10.1029/2005GL025583.

Kam, J., and J. Sheffield, 2016: Increased drought and pluvial risk over California due to changing oceanic conditions. *J. Climate*, **29**, 8269–8279, https://doi.org/10.1175/JCLI-D-15-0879.1.

Koster, R. D., and M. J. Suarez, 1996: Energy and water balance calculations in the Mosaic LSM. NASA Tech. Memo. 104606, Vol. 9, 58 pp.

——, and ——, 2001: Soil moisture memory in climate models. *J. Hydrometeor.*, **2**, 558–570, https://doi.org/10.1175/1525-7541(2001)002<0558:SMMICM>2.0.CO;2.

——, ——, A. Ducharne, M. Stieglitz, and P. Kumar, 2000: A catchment-based approach to modeling land surface processes in a general circulation model 1. Model structure. *J. Geophys. Res.*, **105**, 24 809–24 822, https://doi.org/10.1029/2000JD900327.

——, and Coauthors, 2010: Contribution of land surface initialization to subseasonal forecast skill: First results from a multimodel experiment. *Geophys. Res. Lett.*, **37**, L02402, https://doi.org/10.1029/2009GL041677.

——, and Coauthors, 2011: The second phase of the Global Land–Atmosphere Coupling Experiment: Soil moisture contributions to subseasonal forecast skill. *J. Hydrometeor.*, **12**, 805–822, https://doi.org/10.1175/2011JHM1365.1.

Kumar, S., and V. Merwade, 2011: Evaluation of NARR and CLM3.5 outputs for surface water and energy budgets in the Mississippi River Basin. *J. Geophys. Res.*, **116**, D08115, https://doi.org/10.1029/2010JD014909.

——, D. Lawrence, P. Dirmeyer, and J. Sheffield, 2014a: Less reliable water availability in the 21st century climate projections. *Earth's Future*, **2**, 152–160, https://doi.org/10.1002/2013EF000159.

——, and Coauthors, 2014b: Effects of realistic land surface initializations on subseasonal to seasonal soil moisture and temperature predictability in North America and in changing climate simulated by CCSM4. *J. Geophys. Res. Atmos.*, **119**, 13 250–13 270, https://doi.org/10.1002/2014JD022110.

——, F. Zwiers, P. A. Dirmeyer, D. M. Lawrence, R. Shrestha, and A. T. Werner, 2016: Terrestrial contribution to the heterogeneity in hydrological changes under global warming. *Water Resour. Res.*, **52**, 3127–3142, https://doi.org/10.1002/2016WR018607.

Langford, S., S. Stevenson, and D. Noone, 2014: Analysis of low-frequency precipitation variability in CMIP5 historical simulations for southwestern North America. *J. Climate*, **27**, 2735–2756, https://doi.org/10.1175/JCLI-D-13-00317.1.

Lee, J. E., R. S. Oliveira, T. E. Dawson, and I. Fung, 2005: Root functioning modifies seasonal climate. *Proc. Natl. Acad. Sci. USA*, **102**, 17 576–17 581, https://doi.org/10.1073/pnas.0508785102.

Liang X., D. P. Lettenmaier, E. F. Wood, and S. J. Burges, 1994: A simple hydrologically based model of land surface water and energy fluxes for general circulation models. *J. Geophys. Res.*, **99**, 14 415–14 428, https://doi.org/10.1029/94JD00483.

Livneh, B., and M. P. Hoerling, 2016: The physics of drought in the U.S. central Great Plains. *J. Climate*, **29**, 6783–6804, https://doi.org/10.1175/JCLI-D-15-0697.1.

——, and Coauthors, 2013: A long-term hydrologically based dataset of land surface fluxes and states for the conterminous United States: Update and extensions. *J. Climate*, **26**, 9384–9392, https://doi.org/10.1175/JCLI-D-12-00508.1.

——, R. Kumar, and L. Samaniego, 2015a: Influence of soil textural properties on hydrologic fluxes in the Mississippi River basin. *Hydrol. Processes*, **29**, 4638–4655, https://doi.org/10.1002/hyp.10601.

——, T. J. Bohn, D. W. Pierce, F. Munoz-Arriola, B. Nijssen, R. Vose, D. R. Cayan, and L. Brekke, 2015b: A spatially comprehensive, hydrometeorological data set for Mexico, the U.S., and Southern Canada 1950–2013. *Sci. Data*, **2**, 150042, https://doi.org/10.1038/sdata.2015.42.

Lyon, B., and R. M. Dole, 1995: A diagnostic comparison of the 1980 and 1988 U.S. summer heat wave-droughts. *J. Climate*, **8**, 1658–1675, https://doi.org/10.1175/1520-0442(1995)008<1658:ADCOTA>2.0.CO;2.

Mahanama, S., B. Livneh, R. Koster, D. Lettenmaier, and R. Reichle, 2012: Soil moisture, snow, and seasonal streamflow

forecasts in the United States. *J. Hydrometeor.*, **13**, 189–203, https://doi.org/10.1175/JHM-D-11-046.1.

Mantua, N. J., S. R. Hare, Y. Zhang, J. M. Wallace, and R. C. Francis, 1997: A Pacific interdecadal climate oscillation with impacts on salmon production. *Bull. Amer. Meteor. Soc.*, **78**, 1069–1079, https://doi.org/10.1175/1520-0477(1997)078<1069: APICOW>2.0.CO;2.

Markewitz, D., S. Devine, E. A. Davidson, P. Brando, and D. C. Nepstad, 2010: Soil moisture depletion under simulated drought in the Amazon: Impacts on deep root uptake. *New Phytol.*, **187**, 592–607, https://doi.org/10.1111/j.1469-8137.2010.03391.x.

Martens, B., and Coauthors, 2017: GLEAM v3: Satellite-based land evaporation and root-zone soil moisture. *Geosci. Model Dev.*, **10**, 1903–1925, https://doi.org/10.5194/gmd-10-1903-2017.

Matsumura, S., and K. Yamazaki, 2012: A longer climate memory carried by soil freeze–thaw processes in Siberia. *Environ. Res. Lett.*, **7**, 045402, https://doi.org/10.1088/1748-9326/7/4/045402.

McCabe, G. J., M. A. Palecki, and J. L. Betancourt, 2004: Pacific and Atlantic Ocean influences on multidecadal drought frequency in the United States. *Proc. Natl. Acad. Sci. USA*, **101**, 4136–4141, https://doi.org/10.1073/pnas.0306738101.

Meinzer, F. C., J. R. Brooks, S. Bucci, G. Goldstein, F. G. Scholz, and J. M. Warren, 2004: Converging patterns of uptake and hydraulic redistribution of soil water in contrasting woody vegetation types. *Tree Physiol.*, **24**, 919–928, https://doi.org/10.1093/treephys/24.8.919.

Miguez-Macho, G., and Y. Fan, 2012: The role of groundwater in the Amazon water cycle: 2. Influence on seasonal soil moisture and evapotranspiration. *J. Geophys. Res.*, **117**, D15114, https://doi.org/10.1029/2012JD017540.

Mo, K. C., and D. P. Lettenmaier, 2015: Heat wave flash droughts in decline. *Geophys. Res. Lett.*, **42**, 2823–2829, https://doi.org/10.1002/2015GL064018.

Namias, J., and R. M. Born, 1970: Temporal coherence in North Pacific sea-surface temperature patterns. *J. Geophys. Res.*, **75**, 5952–5955, https://doi.org/10.1029/JC075i030p05952.

Neumann, R. B., and Z. G. Cardon, 2012: The magnitude of hydraulic redistribution by plant roots: A review and synthesis of empirical and modeling studies. *New Phytol.*, **194**, 337–352, https://doi.org/10.1111/j.1469-8137.2012.04088.x.

Newman, M., G. P. Compo, and M. A. Alexander, 2003: ENSO-forced variability of the Pacific decadal oscillation. *J. Climate*, **16**, 3853–3857, https://doi.org/10.1175/1520-0442(2003)016<3853: EVOTPD>2.0.CO;2.

——, and Coauthors, 2016: The Pacific decadal oscillation, revisited. *J. Climate*, **29**, 4399–4427, https://doi.org/10.1175/JCLI-D-15-0508.1.

Nicolai-Shaw, N., L. Gudmundsson, M. Hirschi, and S. I. Seneviratne, 2016: Long-term predictability of soil moisture dynamics at the global scale: Persistence versus large-scale drivers. *Geophys. Res. Lett.*, **43**, 8554–8562, https://doi.org/10.1002/2016GL069847.

Oglesby, R. J., and D. J. Erickson, 1989: Soil moisture and the persistence of North American drought. *J. Climate*, **2**, 1362–1380, https://doi.org/10.1175/1520-0442(1989)002<1362: SMATPO>2.0.CO;2.

Oleson, and Coauthors, 2013: Technical description of version 4.5 of the Community Land Model (CLM). NCAR Tech. Note NCAR/TN-503+STR, 420 pp, https://doi.org/10.5065/D6RR1W7M.

Orth, R., and S. I. Seneviratne, 2012: Analysis of soil moisture memory from observations in Europe. *J. Geophys. Res.*, **117**, D15115, https://doi.org/10.1029/2011JD017366.

——, and ——, 2013: Predictability of soil moisture and streamflow on subseasonal timescales: A case study. *J. Geophys. Res. Atmos.*, **118**, 10 963–10 979, https://doi.org/10.1002/jgrd.50846.

——, R. D. Koster, and S. I. Seneviratne, 2013: Inferring soil moisture memory from streamflow observations using a simple water balance model. *J. Hydrometeor.*, **14**, 1773–1790, https://doi.org/10.1175/JHM-D-12-099.1.

Otkin, J. A., and Coauthors, 2016: Assessing the evolution of soil moisture and vegetation conditions during the 2012 United States flash drought. *Agric. For. Meteor.*, **218–219**, 230–242, https://doi.org/10.1016/j.agrformet.2015.12.065.

PaiMazumder, D., and J. M. Done, 2016: Potential predictability sources of the 2012 US drought in observations and a regional model ensemble. *J. Geophys. Res. Atmos.*, **121**, 12 581–12 592, https://doi.org/10.1002/2016JD025322.

Paolino, D. A., J. L. Kinter, B. P. Kirtman, D. H. Min, and D. M. Straus, 2012: The impact of land surface and atmospheric initialization on seasonal forecasts with CCSM. *J. Climate*, **25**, 1007–1021, https://doi.org/10.1175/2011JCLI3934.1.

Quiring, S. M., T. W. Ford, J. K. Wang, A. Khong, E. Harris, T. Lindgren, D. W. Goldberg, and Z. Li, 2016: The North American Soil Moisture Database: Development and applications. *Bull. Amer. Meteor. Soc.*, **97**, 1441–1459, https://doi.org/10.1175/BAMS-D-13-00263.1.

Rahman, M. M., M. J. Lu, and K. H. Kyi, 2015: Variability of soil moisture memory for wet and dry basins. *J. Hydrol.*, **523**, 107–118, https://doi.org/10.1016/j.jhydrol.2015.01.033.

Reichle, R. H., C. S. Draper, Q. Liu, M. Girotto, S. P. P. Mahanama, R. D. Koster, and G. J. M. De Lannoy, 2017: Assessment of MERRA-2 land surface hydrology estimates. *J. Climate*, **30**, 2937–2960, https://doi.org/10.1175/JCLI-D-16-0720.1.

Rizzo, G., J. I. R. Edreira, S. V. Archontoulis, H. S. Yang, and P. Grassini, 2018: Do shallow water tables contribute to high and stable maize yields in the US Corn Belt? *Global Food Secur.*, **18**, 27–34, https://doi.org/10.1016/j.gfs.2018.07.002.

Routson, C. C., C. A. Woodhouse, J. T. Overpeck, J. L. Betancourt, and N. P. McKay, 2016: Teleconnected ocean forcing of western North American droughts and pluvials during the last millennium. *Quat. Sci. Rev.*, **146**, 238–250, https://doi.org/10.1016/j.quascirev.2016.06.017.

Ryel, R. J., M. M. Caldwell, C. K. Yoder, D. Or, and A. J. Leffler, 2002: Hydraulic redistribution in a stand of *Artemisia tridentata*: Evaluation of benefits to transpiration assessed with a simulation model. *Oecologia*, **130**, 173–184, https://doi.org/10.1007/s004420100794.

——, ——, A. J. Leffler, and C. K. Yoder, 2003: Rapid soil moisture recharge to depth by roots in a stand of *Artemisia tridentata*. *Ecology*, **84**, 757–764, https://doi.org/10.1890/0012-9658(2003)084[0757:RSMRTD]2.0.CO;2.

Scanlon, B. R., 1992: Evaluation of liquid and vapor water flow in desert soils based on chlorine 36 and tritium tracers and nonisothermal flow simulations. *Water Resour. Res.*, **28**, 285–297, https://doi.org/10.1029/91WR02200.

——, and P. C. D. Milly, 1994: Water and heat fluxes in desert soils: 2. Numerical simulations. *Water Resour. Res.*, **30**, 721–733, https://doi.org/10.1029/93WR03252.

Schaefer, G. L., and R. F. Paetzold, 2001: SNOTEL (SNOwpack TELemetry) and SCAN (Soil Climate Analysis Network). Automated Weather Stations for Applications in Agriculture and Water Resources Management: Current Use and Future Perspectives, K. G. Hubbard and M. V. K. Sivakumar, Eds., WMO/TD-1074, 187–194.

——, M. H. Cosh, and T. J. Jackson, 2007: The USDA Natural Resources Conservation Service Soil Climate Analysis Network (SCAN). *J. Atmos. Oceanic Technol.*, **24**, 2073–2077, https://doi.org/10.1175/2007JTECHA930.1.

Schaefer, K. M., T. Zhang, P. P. Tans, and R. Stöckli, 2007: Temperature anomaly reemergence in seasonally frozen soils. *J. Geophys. Res.*, **112**, D20102, https://doi.org/10.1029/2007JD008630.

Schlosser, C. A., and P. C. D. Milly, 2002: A model-based investigation of soil moisture predictability and associated climate predictability. *J. Hydrometeor.*, **3**, 483–501, https://doi.org/10.1175/1525-7541(2002)003<0483:AMBIOS>2.0.CO;2.

Schubert, S. D., M. J. Suarez, P. J. Pegion, R. D. Koster, and J. T. Bacmeister, 2004: Causes of long-term drought in the US Great Plains. *J. Climate*, **17**, 485–503, https://doi.org/10.1175/1520-0442(2004)017<0485:COLDIT>2.0.CO;2.

——, ——, ——, ——, and ——, 2008: Potential predictability of long-term drought and pluvial conditions in the U.S. Great Plains. *J. Climate*, **21**, 802–816, https://doi.org/10.1175/2007JCLI1741.1.

——, and Coauthors, 2016: Global meteorological drought: A synthesis of current understanding with a focus on SST drivers of precipitation deficits. *J. Climate*, **29**, 3989–4019, https://doi.org/10.1175/JCLI-D-15-0452.1.

Seager, R., Y. Kushnir, C. Herweijer, N. Naik, and J. Velez, 2005: Modeling of tropical forcing of persistent droughts and pluvials over western North America: 1856–2000. *J. Climate*, **18**, 4065–4088, https://doi.org/10.1175/JCLI3522.1.

——, N. Graham, C. Herweijer, A. L. Gordon, Y. Kushnir, and E. Cook, 2007: Blueprints for medieval hydroclimate. *Quat. Sci. Rev.*, **26**, 2322–2336, https://doi.org/10.1016/j.quascirev.2007.04.020.

——, R. Burgman, Y. Kushnir, A. Clement, E. Cook, N. Naik, and J. Miller, 2008: Tropical Pacific forcing of North American medieval megadroughts: Testing the concept with an atmosphere model forced by coral-reconstructed SSTs. *J. Climate*, **21**, 6175–6190, https://doi.org/10.1175/2008JCLI2170.1.

——, M. Hoerling, S. Schubert, H. Wang, B. Lyon, A. Kumar, J. Nakamura, and N. Henderson, 2015: Causes of the 2011–14 California drought. *J. Climate*, **28**, 6997–7024, https://doi.org/10.1175/JCLI-D-14-00860.1.

Seneviratne, S. I., and R. D. Koster, 2012: A revised framework for analyzing soil moisture memory in climate data: Derivation and interpretation. *J. Hydrometeor.*, **13**, 404–412, https://doi.org/10.1175/JHM-D-11-044.1.

——, and Coauthors, 2006: Soil moisture memory in AGCM simulations: Analysis of Global Land–Atmosphere Coupling Experiment (GLACE) data. *J. Hydrometeor.*, **7**, 1090–1112, https://doi.org/10.1175/JHM533.1.

Sheffield, J., and Coauthors, 2013: North American climate in CMIP5 experiments. Part I: Evaluation of historical simulations of continental and regional climatology. *J. Climate*, **26**, 9209–9245, https://doi.org/10.1175/JCLI-D-12-00592.1.

Solomon, A., L. and Coauthors, 2011: Distinguishing the roles of natural and anthropogenically forced decadal climate variability. *Bull. Amer. Meteor. Soc.*, **92**, 141–156, https://doi.org/10.1175/2010BAMS2962.1.

Stevenson, S., A. Timmermann, Y. Chikamoto, S. Langford, and P. DiNezio, 2015: Stochastically generated North American megadroughts. *J. Climate*, **28**, 1865–1880, https://doi.org/10.1175/JCLI-D-13-00689.1.

Thornton, P. E., and N. A. Rosenbloom, 2005: Ecosystem model spin-up: Estimating steady state conditions in a coupled terrestrial carbon and nitrogen cycle model. *Ecol. Modell.*, **189**, 25–48, https://doi.org/10.1016/j.ecolmodel.2005.04.008.

——, and Coauthors, 2002: Modeling and measuring the effects of disturbance history and climate on carbon and water budgets in evergreen needleleaf forests. *Agric. For. Meteor.*, **113**, 185–222, https://doi.org/10.1016/S0168-1923(02)00108-9.

Tobin, K. J., R. Torres, W. T. Crow, and M. E. Bennett, 2017: Multi-decadal analysis of root-zone soil moisture applying the exponential filter across CONUS. *Hydrol. Earth Syst. Sci.*, **21**, 4403–4417, https://doi.org/10.5194/hess-21-4403-2017.

van den Dool, H., J. Huang, and Y. Fan, 2003: Performance and analysis of the constructed analogue method applied to U.S. soil moisture over 1981–2001. *J. Geophys. Res.*, **108**, 8617, https://doi.org/10.1029/2002JD003114.

Vinnikov, K. Y., A. Robock, N. A. Speranskaya, and A. Schlosser, 1996: Scales of temporal and spatial variability of midlatitude soil moisture. *J. Geophys. Res.*, **101**, 7163–7174, https://doi.org/10.1029/95JD02753.

Viovy, N., and P. Ciais, 2011: CRUNCEP data set for 1901–2008. ftp://nacp.ornl.gov/synthesis/2009/frescati/temp/land_use_change/original/readme.htm.

Wood, A. W., T. Hopson, A. Newman, L. Brekke, J. Arnold, and M. Clark, 2016: Quantifying streamflow forecast skill elasticity to initial condition and climate prediction skill. *J. Hydrometeor.*, **17**, 651–668, https://doi.org/10.1175/JHM-D-14-0213.1.

Woodhouse, C. A., and J. T. Overpeck, 1998: 2000 years of drought variability in the central United States. *Bull. Amer. Meteor. Soc.*, **79**, 2693–2714, https://doi.org/10.1175/1520-0477(1998)079<2693:YODVIT>2.0.CO;2.

Wu, R., and J. L. Kinter III, 2009: Analysis of the relationship of U.S. droughts with SST and soil moisture: Distinguishing the time scale of droughts. *J. Climate*, **22**, 4520–4538, https://doi.org/10.1175/2009JCLI2841.1.

Wu, W., and R. E. Dickinson, 2004: Time scales of layered soil moisture memory in the context of land–atmosphere interaction. *J. Climate*, **17**, 2752–2764, https://doi.org/10.1175/1520-0442(2004)017<2752:TSOLSM>2.0.CO;2.

——, M. A. Geller, and R. E. Dickinson, 2002: The response of soil moisture to long-term variability of precipitation. *J. Hydrometeor.*, **3**, 604–613, https://doi.org/10.1175/1525-7541(2002)003<0604:TROSMT>2.0.CO;2.

Xia, Y. L., and Coauthors, 2012: Continental-scale water and energy flux analysis and validation for the North American Land Data Assimilation System project phase 2 (NLDAS-2): 1. Intercomparison and application of model products. *J. Geophys. Res.*, **117**, D03109, https://doi.org/10.1029/2011JD016048.

——, and Coauthors, 2014: Evaluation of multi-model simulated soil moisture in NLDAS-2. *J. Hydrol.*, **512**, 107–125, https://doi.org/10.1016/j.jhydrol.2014.02.027.

Yan, B. Y., and R. E. Dickinson, 2014: Modeling hydraulic redistribution and ecosystem response to droughts over the Amazon basin using Community Land Model 4.0 (CLM4). *J. Geophys. Res. Biogeosci.*, **119**, 2130–2143, https://doi.org/10.1002/2014JG002694.

Yang, S., X. Ding, D. Zheng, and Q. Li, 2007: Depiction of the variations of Great Plains precipitation and its relationship with tropical central-eastern Pacific SST. *J. Appl. Meteor. Climatol.*, **46**, 136–153, https://doi.org/10.1175/JAM2455.1.

Zeng, X. B., 2001: Global vegetation root distribution for land modeling. *J. Hydrometeor.*, **2**, 525–530, https://doi.org/10.1175/1525-7541(2001)002<0525:GVRDFL>2.0.CO;2.